Quantum calculations for rotational energy transfer in nitrogen molecule collisions

Winifred M. Huo

NASA Ames Research Center, Moffett Field, CA 94035-1000

Sheldon Green

NASA Goddard Space Flight Center, Institute for Space Studies, New York, New York 10025

(November 29, 1995)

Abstract

Rotational energy transfer in collisions of nitrogen molecules has been studied theoretically, using the N_2-N_2 rigid-rotor potential of van der Avoird, et al. [J. Chem. Phys. **84**, 1629 (1986)]. For benchmarking purposes, converged close coupling (CC) calculations have been carried out to a total energy of about 200 cm^{-1}. Coupled states (CS) approximation calculations have been carried out to a total energy of 680 cm^{-1}, and infinite order sudden (IOS) approximation calculations have also been carried out. The CC and CS cross sections have been obtained both with and without identical molecule exchange symmetry, whereas exchange was neglected in the IOS calculations. The CS results track the CC cross sections rather well: between 113 - 219 cm^{-1} the average deviation is 14%, with accuracy improving at higher energy. Comparison between the CS and IOS cross sections at the high energy end of the CS calculations, 500 - 680 cm^{-1}, shows that IOS is sensitive to the amount of inelasticity and the results for large ΔJ transitions are subject to larger errors. State-to-state cross sections with even and odd exchange symmetry agree to better than 2% and are well represented as a sum of direct and

exchange cross sections for distinguishable molecules, an indication of the applicability of a classical treatment for this system. This result, however, does not apply to partial cross sections for given total J, but arises from a near cancellation of the interference terms between even and odd exchange symmetries on summing over partial waves. In order to compare with experimental data for rotational excitation rates of N_2 in the n=1 excited vibrational level colliding with ground vibrational level (n=0) bath N_2 molecules, it is assumed that exchange scattering between molecules in different vibrational levels is negligible and direct scattering is independent of n so that distinguishable molecule rigid rotor rates may be used. With these assumptions good agreement is obtained. Although the IOS approximation itself is found to provide only moderately accurate values for rate constants, IOS/ECS scaling methods, especially if based on fundamental rates obtained from coupled channel results, are found to provide generally good accuracy.

I. INTRODUCTION

Being the most abundant species in the air, ro-vibrational excitation/deexcitation in N_2 collisions dominates the thermalization process when excess energy is supplied, for example, in hypersonic flow fields, wind tunnels, or arc jets. In the velocity regime where the flow is characterized by different rotational, vibrational, and electronic temperatures, [1] i.e., the so called nonequilibrium regime, detailed knowledge of relative rates for intramolecular and intermolecular energy transfer among vibrational (V), rotational (R), and translational (T) degrees of freedom is required to determine the time it takes for the flow field to re-establish equilibrium. These energy transfer rates are also required in modeling the operation of lasers and other processes which require the knowledge of energy deposition pathways in air.

In spite of the importance of energy transfer rates in N_2, few direct experimental measurements are available, and most studies rely on simple models to deduce the rate constants.

A notable exception is the work of Sitz and Farrow. [2] Using a pump-probe technique, they directly determined rotational energy transfer rates of N_2 in the excited, $n = 1$ vibrational level upon collision with a bath of N_2 molecules in the ground, $n = 0$, vibrational level. Analogous studies on vibrational energy transfer are not available. Another quantity closely related to rotational excitation rates is the collisionally induced spectral line shape. Line shapes in coherent anti-Stokes Raman spectra (CARS) and stimulated Raman spectra (SRS) of the vibrational Q-branch of N_2 are widely used as a temperature probe for spatially and temporally inhomogeneous environments and this has prompted many studies of R-R and R-T collisional energy transfer in this system. Comparison of theoretical results from the present calculations with linewidth data will be treated in a separate paper. [3]

Theoretically, much effort has been devoted to the modeling of these energy transfer processes. However, studies of V-V transfer neglected rotation, and most studies of R-R and R-T transfer used a very simple potential energy surface and/or employed various approximations to simplify the dynamics. Koszykowski, et al. [4] employed an atom-atom pairwise additive Lennard-Jones potential and determined the rate constants using quasi-classical trajectory calculations. While the goal of their calculations was to determine Raman linewidths, they also deduced a scaling law for the rotational excitation rate constants. Using a somewhat improved interaction potential, Agg and Clary [5] reported rotational excitation rate constants calculated with the quantum mechanical infinite order sudden (IOS) approximation and also with a modified breathing sphere approximation. Billing and Wang [6] used a semi-classical scattering formalism along with a simple pairwise additive exponential repulsive interaction to calculate high temperature rotational relaxation and transport coefficients. The most accurate rigid-rotor N_2-N_2 potential reported so far is that of van der Avoird, et al. [7] (vdA) which is based on ab initio calculations and adjusted to fit the second virial coefficients. Using the vdA potential, Green [8] determined the R-R transfer rates using the IOS approximation and the energy corrected sudden (ECS) approximation, obtaining reasonable agreement with experiment. Also using the vdA potential, Heck and Dickinson [9] used classical trajectory scattering calculations to obtain transport and relaxation cross

sections, finding good agreement with the former but an inconsistent pattern for the latter which they interpreted as suggesting that the interaction may be insufficiently anisotropic in regions sampled at low energy.

The present study also employed the vdA potential, but used accurate close coupling (CC) scattering calculations as well as approximate quantum dynamical treatments. To test the range of validity of different angular momentum decoupling schemes, we carried out collision calculations using the essentially exact CC formulation and the coupled states (CS) approximation, also called the centrifugal sudden approximation, to as high an energy as our resources would allow. In addition, the IOS approximation was employed.

The role of identical molecule exchange symmetry is of much interest. All previous calculations on this system neglected this symmetry. In the present work, the CC and CS cross sections were obtained both with and without exchange symmetry to better understand the role of this process and to help devise economical schemes to treat ro-vibrational excitation. There appears to be some inconsistency in the literature concerning degeneracy factors for computing cross sections for indistinguishable molecules. It is important that this degeneracy factor is consistent with counting of states in the two-body density matrix. We use here a different convention from the widely used formula of Takayanagi, [10] and this is discussed in some detail in the next Section. Results of the present calculation are then presented in Section III. Section III A considers the accuracy of the CS approximation by comparing with CC results and the accuracy of the IOS approximation by comparing with CS results; III B examines the role of identical molecule exchange symmetry; and III C compares the rotational excitation rate constants obtained by the different approximations with experimental values. Finally, we present a brief summary in Section IV.

II. COLLISIONS BETWEEN IDENTICAL MOLECULES

When the colliding system is composed of identical molecules, the symmetry of the wave function under exchange must be taken into account. Early treatments of exchange were

given by Takayanagi, [11] Gioumousis and Curtiss, [12] and Davison. [13] The cross section expression of Takayanagi [10] has been commonly used in the literature for the collision of identical molecules and is incorporated in the MOLSCAT [14] computer code. However, a re-examination of the derivation of this expression indicates a problem with normalization and symmetrization of the asymptotic wave function that was used to deduce the scattering amplitude. Indeed, if one uses a normalized incoming flux and an outgoing flux where the two molecules maintain proper exchange symmetry, the cross section so derived is different from Takayanagi's. Because this has not been discussed in the literature, we rederive below the cross section expression using properly normalized and symmetrized asymptotic wave functions and compare the result with Takayanagi's expression and other expressions used in the literature.

Let n_1, j_1, m_1 and n_2, j_2, m_2 denote the initial vibrational and rotational quantum numbers of the two molecules. The asymptotic form of the symmetrized wave function $\Psi^{\pm}$ under the incoming plane wave and outgoing spherical wave boundary condition is

$$\begin{aligned}
\lim_{R\to\infty} \Psi^{\pm} \to & \frac{1}{\sqrt{2(1+\delta_{n_1 n_2}\delta_{j_1 j_2}\delta_{m_1 m_2})}} \\
& \times \{\exp(i\mathbf{k}_\alpha \cdot \mathbf{R})\chi_{n_1 j_1}(r_1)Y_{j_1 m_1}(\hat{r}_1)\chi_{n_2 j_2}(r_2)Y_{j_2 m_2}(\hat{r}_2) \\
& \pm \exp(-i\mathbf{k}_\alpha \cdot \mathbf{R})\chi_{n_1 j_1}(r_2)Y_{j_1 m_1}(\hat{r}_2)\chi_{n_2 j_2}(r_1)Y_{j_2 m_2}(\hat{r}_1)\} \\
& + \sum_{\alpha'}{}' \sum_{m_1'}{}' \sum_{m_2'}{}' \frac{i}{(k_\alpha k_{\alpha'})^{\frac{1}{2}}} \frac{\exp(ik_{\alpha'}R)}{R} \frac{1}{\sqrt{2(1+\delta_{n_1' n_2'}\delta_{j_1' j_2'}\delta_{m_1' m_2'})}} \\
& \times \{q(n_1' j_1' m_1' n_2' j_2' m_2'|\hat{R})\chi_{n_1' j_1'}(r_1)Y_{j_1' m_1'}(\hat{r}_1)\chi_{n_2' j_2'}(r_2)Y_{j_2' m_2'}(\hat{r}_2) \\
& \pm q(n_1' j_1' m_1' n_2' j_2' m_2'|-\hat{R})\chi_{n_1' j_1'}(r_2)Y_{j_1' m_1'}(\hat{r}_2)\chi_{n_2' j_2'}(r_1)Y_{j_2' m_2'}(\hat{r}_1)\}. \qquad (2.1)
\end{aligned}$$

Here $\mathbf{r}_i = (r_i, \hat{r}_i)$ is the vector, in the space-fixed, center of mass coordinate system, between the two nuclei in molecule i; and $\mathbf{R}$, the vector from the center of mass of molecule 1 to that of molecule 2. Also, $\mathbf{k}_\alpha$ is the wave vector of relative motion, and $\chi_{nj}(r)$ and $Y_{jm}(\hat{r})$ the vibrational and rotational wave functions. The superscript $\pm$ denotes the system being symmetric or antisymmetric with respect to the interchange of the two molecules, and α' denotes the collection of quantum numbers n_1', n_2', j_1', j_2'. In Eq. (2.1) the summations over

α', m_1', and m_2' are restricted to the range,

$$\begin{aligned} &n_1 > n_2, \text{ all } j_1, j_2, m_1, m_2; \\ &n_1 = n_2, \ j_1 > j_2, \text{ all } m_1, m_2; \\ &n_1 = n_2, \ j_1 = j_2, \ m_1 \geq m_2; \end{aligned} \tag{2.2}$$

and this restriction is indicated by the primes on the summation symbols. The first term in Eq. (2.1) gives a symmetrized and δ-function normalized incoming plane wave. In the second term, exchange symmetry is maintained in the ro-vibrational wave functions associated with the outgoing spherical wave. The scattering amplitude is determined by $q(n_1'j_1'm_1'n_2'j_2'm_2'|\hat{R})$ and $q(n_1'j_1'm_1'n_2'j_2'm_2'|-\hat{R})$.

Most calculations, the present included, do not determine $q(n_1'j_1'm_1'n_2'j_2'm_2'|\hat{R})$ and $q(n_1'j_1'm_1'n_2'j_2'm_2'|-\hat{R})$ directly. Instead, calculations are carried out in the total angular momentum (J) representation because the set of coupled equations for the collision problem is block diagonal in J and independent of M, the projection of J on the space-fixed Z-axis, leading to much smaller calculations. A properly symmetrized and normalized basis to expand the wave function of the colliding system, $\Psi^{\pm}$, is then

$$I^{\pm}_{JM}(\alpha j_{12} l|\hat{R}, \mathbf{r}_1, \mathbf{r}_2) = \frac{1}{\sqrt{2(1+\delta_{n_1 n_2}\delta_{j_1 j_2})}}\{I_{JM}(\alpha j_{12} l|\hat{R}, \mathbf{r}_1, \mathbf{r}_2) \pm I_{JM}(\alpha j_{12} l|-\hat{R}, \mathbf{r}_2, \mathbf{r}_1)\}, \tag{2.3}$$

with

$$I_{JM}(\alpha j_{12} l|\hat{R}, \mathbf{r}_1, \mathbf{r}_2) = \chi_{n_1 j_1}(r_1)\chi_{n_2 j_2}(r_2)\mathcal{Y}_{JM}(\hat{R}, \hat{r}_1, \hat{r}_2). \tag{2.4}$$

Here l is the angular momentum of relative motion, $\mathbf{j_{12}} = \mathbf{j}_1 + \mathbf{j}_2$, and $\mathbf{J} = \mathbf{l} + \mathbf{j_{12}}$. The coupled angular momentum function $\mathcal{Y}_{JM}$ can be expressed in terms of the uncoupled functions

$$\begin{aligned} \mathcal{Y}_{JM}(\hat{R}, \hat{r}_1, \hat{r}_2) = \sum_{m_1}\sum_{m_2}&(j_1 j_2 m_1 m_2|j_1 j_2 j_{12}\ m_1+m_2)(j_{12} l\ m_1+m_2\ M-m_1-m_2|j_{12} l J M) \\ &\times Y_{l\ M-m_1-m_2}(\hat{R}) Y_{j_1 m_1}(\hat{r}_1) Y_{j_2 m_2}(\hat{r}_2). \end{aligned} \tag{2.5}$$

where $(j_1 j_2 m_1 m_2|j_1 j_2 j_{12} m_{12})$ is the vector coupling coefficients as defined by Condon and Shortley. [15] Note that the summation over m_1, m_2 in Eq. (2.5), arising from the expansion

of the coupled angular momentum function $\mathcal{Y}_{JM}$ in terms of the uncoupled functions, is over the complete range of m_1 and m_2. Using the relations,

$$(j_1 j_2 m_1 m_2 | j_1 j_2 j_{12}\ m_1+m_2) = (-1)^{j_1+j_2+j_{12}} (j_2 j_1 m_2 m_1 | j_2 j_1 j_{12}\ m_1+m_2), \tag{2.6}$$

and

$$Y_{l\nu}(\hat{R}) = (-1)^l Y_{l\nu}(-\hat{R}), \tag{2.7}$$

Eq. (2.3) can be written as

$$\begin{aligned} I^{\pm}_{JM}(n_1 n_2 j_1 j_2 j_{12} l | \hat{R}, \mathbf{r}_1, \mathbf{r}_2) = & \frac{1}{\sqrt{2(1+\delta_{n_1 n_2}\delta_{j_1 j_2})}} \{ I_{JM}(n_1 n_2 j_1 j_2 j_{12} l | \hat{R}, \mathbf{r}_1, \mathbf{r}_2) \\ & \pm (-1)^{j_1+j_2+j_{12}+l} I_{JM}(n_2 n_1 j_2 j_1 j_{12} l | \hat{R}, \mathbf{r}_1, \mathbf{r}_2) \}. \end{aligned} \tag{2.8}$$

The asymptotic form of the scattering wave function $\Psi^{\pm}$ in the J-representation is given by

$$\begin{aligned} \lim_{R\to\infty} \Psi^{\pm} \to & \sum_J \sum_M \sum_{j_{12}} \sum_l A_{JM}(\alpha j_{12} l; k_\alpha) \sum_{\alpha'} {}' \sum_{j'_{12}} \sum_{l'} \\ & \times \Big\{ \delta(\alpha j_{12} l; \alpha' j'_{12} l') [\exp(-i(k_\alpha R - \frac{1}{2} l\pi)) - \exp(i(k_\alpha R - \frac{1}{2} l\pi))]/R \\ & + [\delta(\alpha j_{12} l; \alpha' j'_{12} l') - S^{\pm}_J(\alpha j_{12} l; \alpha' j'_{12} l')] (\frac{k_\alpha}{k_{\alpha'}})^{\frac{1}{2}} \exp[i(k_{\alpha'} R - \frac{1}{2} l'\pi)]/R \Big\} \\ & \times I^{\pm}_{JM}(\alpha' j'_{12} l' | \hat{R}, \mathbf{r}_1, \mathbf{r}_2). \end{aligned} \tag{2.9}$$

The coefficient $A_{JM}(\alpha j_{12} l; k_\alpha)$ is determined by equating the first terms on the right hand side of Eq. (2.1) and Eq. (2.9), both representing the incoming wave:

$$\begin{aligned} A_{JM}(\alpha j_{12} l; k_\alpha) = & -4\pi \frac{i^l}{2ik_\alpha} \left(\frac{1+\delta_{n_1 n_2}\delta_{j_1 j_2}}{1+\delta_{n_1 n_2}\delta_{j_1 j_2}\delta_{m_1 m_2}} \right)^{\frac{1}{2}} Y^*_{l\, M-m_1-m_2}(\Theta_o \Phi_o) \\ & \times (j_1 j_2 m_1 m_2 | j_1 j_2 j_{12}\ m_1+m_2)(l j_{12}\ M-m_1-m_2\ m_1+m_2 | l j_{12} J M), \end{aligned} \tag{2.10}$$

with Θ_o, Φ_o the angular coordinates of $\mathbf{k}_\alpha$.

The factor $[(1+\delta_{n_1 n_2}\delta_{j_1 j_2})/(1+\delta_{n_1 n_2}\delta_{j_1 j_2}\delta_{m_1 m_2})]^{\frac{1}{2}}$ in Eq. (2.10) accounts for the difference in the manner in which the J-representation and the uncoupled representation treat m_1 and m_2 when $n_1 = n_2$ and $j_1 = j_2$. In the uncoupled representation, the asymptotic expression

for $\Psi^{\pm}$ in Eq. (2.1) accounts for the fact that the internal state wave functions of the two molecules are identical only if $n_1 = n_2$, $j_1 = j_2$, and $m_1 = m_2$, and for this case the factor $(1 + \delta_{n_1 n_2}\delta_{j_1 j_2}\delta_{m_1 m_2})^{-\frac{1}{2}}$ is required to normalize the symmetrized ro-vibrational wave function properly. The J-representation does not depend explicitly on m_1 or m_2 and, in fact, requires a complete sum over m_1 and m_2, even when $n_1 = n_2$ and $j_1 = j_2$. Therefore, the normalization for $\Psi^{\pm}$ in the J-representation is $(1 + \delta_{n_1 n_2}\delta_{j_1 j_2})^{-\frac{1}{2}}$ and the conditions analogous to Eq. (2.2) are

$$\begin{aligned} & n_1 > n_2, \text{ all } j_1, j_2; \\ & n_1 = n_2, \ j_1 \geq j_2. \end{aligned} \tag{2.11}$$

In terms of the uncoupled representation this constitutes a double counting of some m_1, m_2 states and it is necessary to account for this when transforming the J-representation S-matrices back to the uncoupled basis in order to obtain scattering amplitudes and cross sections.

Equating the second term on the right hand side of Eq. (2.1), representing the outgoing spherical wave, with the second term in Eq. (2.9) gives the expression for $q(n_1' j_1' m_1' n_2' j_2' m_2'|\hat{R})$:

$$\begin{aligned} q(n_1' j_1' m_1' n_2' j_2' m_2'|\hat{R}) = 2\pi \sum_J \sum_M \sum_{j_{12}} \sum_{j_{12}'} \sum_l \sum_{l'} i^{l-l'} \\ \times \left(\frac{(1 + \delta_{n_1 n_2}\delta_{j_1 j_2})(1 + \delta_{n_1' n_2'}\delta_{j_1' j_2'})}{(1 + \delta_{n_1 n_2}\delta_{j_1 j_2}\delta_{m_1 m_2})(1 + \delta_{n_1' n_2'}\delta_{j_1' j_2'}\delta_{m_1' m_2'})} \right)^{\frac{1}{2}} Y^*_{l\, M-m_1-m_2}(\Theta_o \Phi_o) \\ \times (j_1 j_2 m_1 m_2 | j_1 j_2 j_{12}\ m_1 + m_2)(l j_{12}\ M - m_1 - m_2\ m_1 + m_2 | l j_{12} J M) \\ \times T_J^{\pm}(\alpha j_{12} l; \alpha' j_{12}' l')(j_1' j_2' m_1' m_2' | j_1' j_2' j_{12}'\ m_1' + m_2') \\ \times (j_{12}' l'\ m_1' + m_2'\ M - m_1' - m_2' | j_{12}' l' J M) Y_{l'\, M-m_1'-m_2'}(\hat{R}). \end{aligned} \tag{2.12}$$

The T-matrix, $T_J^{\pm}$, is simply related to the S-matrix as

$$T_J^{\pm}(\alpha j_{12} l; \alpha' j_{12}' l') = \delta(\alpha j_{12} l; \alpha' j_{12}' l') - S_J^{\pm}(\alpha j_{12} l; \alpha' j_{12}' l'). \tag{2.13}$$

The expression for $q(n_1' j_1' m_1' n_2' j_2' m_2'|-\hat{R})$ is the same as Eq. (2.12) except that $Y_{l'\, M-m_1'-m_2'}(\hat{R})$ is replaced by $Y_{l'\, M-m_1'-m_2'}(-\hat{R})$.

Substituting the expressions of $q(n_1'j_1'm_1'n_2'j_2'm_2'|\hat{R})$ and $q(n_1'j_1'm_1'n_2'j_2'm_2'|-\hat{R})$ into $\Psi^{\pm}$ in the uncoupled basis and making use of Eqs. (2.6) and (2.7), Eq. (2.1) becomes

$$\begin{aligned}
\lim_{R\to\infty}\Psi^{\pm}\to & \frac{1}{\sqrt{2(1+\delta_{n_1n_2}\delta_{j_1j_2}\delta_{m_1m_2})}} \\
& \times\{\exp(i\mathbf{k}_\alpha\cdot\mathbf{R})\chi_{n_1j_1}(r_1)Y_{j_1m_1}(\hat{r}_1)\chi_{n_2j_2}(r_2)Y_{j_2m_2}(\hat{r}_2) \\
& \pm\exp(-i\mathbf{k}_\alpha\cdot\mathbf{R})\chi_{n_1j_1}(r_2)Y_{j_1m_1}(\hat{r}_2)\chi_{n_2j_2}(r_1)Y_{j_2m_2}(\hat{r}_1)\} \\
& +\sum_{\alpha'}{}'\sum_{m_1'}{}'\sum_{m_2'}{}'\frac{i}{(k_\alpha k_{\alpha'})^{\frac{1}{2}}}\frac{\exp(ik_{\alpha'}R)}{R}\sum_J\sum_M\sum_{j_{12}}\sum_{j_{12}'}\sum_l\sum_{l'} \\
& \times\Big\{2\pi i^{l-l'}Y^*_{l\,M-m_1-m_2}(\Theta_o\Phi_o)\,(j_1j_2m_1m_2|j_1j_2j_{12}\ m_1+m_2) \\
& \times(lj_{12}\ M-m_1-m_2\ m_1+m_2|lj_{12}JM)T^{\pm}_J(\alpha j_{12}l;\alpha'j_{12}'l') \\
& \times(j_1'j_2'm_1'm_2'|j_1'j_2'j_{12}'\ m_1'+m_2')(j_{12}'l'\ m_1'+m_2'\ M-m_1'-m_2'|j_{12}'l'JM)\Big\} \\
& \times Y_{l'\,M-m_1'-m_2'}(\hat{R}) \\
& \times\Big(\frac{1}{2(1+\delta_{n_1'n_2'}\delta_{j_1'j_2'}\delta_{m_1'm_2'})}\Big)^{\frac{1}{2}}\Big(\frac{(1+\delta_{n_1n_2}\delta_{j_1j_2})(1+\delta_{n_1'n_2'}\delta_{j_1'j_2'})}{(1+\delta_{n_1n_2}\delta_{j_1j_2}\delta_{m_1m_2})(1+\delta_{n_1'n_2'}\delta_{j_1'j_2'}\delta_{m_1'm_2'})}\Big)^{\frac{1}{2}} \\
& \times\Big\{\chi_{n_1'j_1'}(r_1)Y_{j_1'm_1'}(\hat{r}_1)\chi_{n_2'j_2'}(r_2)Y_{j_2'm_2'}(\hat{r}_2) \\
& \pm(-1)^{j_1+j_2+j_{12}+l}\chi_{n_1'j_1'}(r_2)Y_{j_1'm_1'}(\hat{r}_2)\chi_{n_2'j_2'}(r_1)Y_{j_2'm_2'}(\hat{r}_1)\Big\}. \qquad (2.14)
\end{aligned}$$

The outgoing spherical wave in Eq. (2.14) is now in the form of a spherical wave times an angular function and a symmetrized ro-vibrational wave function of the two molecules. The differential cross section, $d\sigma^{\pm}$ is readily deduced from Eq. (2.14). Since most experimental measurements use unpolarized molecules and do not measure the final m_1' and m_2', the corresponding $d\sigma^{\pm}$ should be averaged over m_1 and m_2 and summed over m_1' and m_2':

$$\frac{1}{(2j_1+1)(2j_2+1)}\sum_{m_1}{}'\sum_{m_2}{}'\sum_{m_1'}{}'\sum_{m_2'}{}'.$$

The above sum is restricted in order to count only physically distinguishable states. The conversion from a restricted to a full sum cancels out the factor

$$\Big(\frac{(1+\delta_{n_1n_2}\delta_{j_1j_2})(1+\delta_{n_1'n_2'}\delta_{j_1'j_2'})}{(1+\delta_{n_1n_2}\delta_{j_1j_2}\delta_{m_1m_2})(1+\delta_{n_1'n_2'}\delta_{j_1'j_2'}\delta_{m_1'm_2'})}\Big)^{\frac{1}{2}}.$$

Thus $d\sigma^{\pm}$ is given by

$$
\begin{aligned}
d\sigma^{\pm} = & \frac{1}{{k_\alpha}^2}\frac{1}{(2j_1+1)(2j_2+1)}\sum_{m_1}\sum_{m_2}\sum_{m_1'}\sum_{m_2'} \\
& |2\pi\sum_{J}\sum_{M}\sum_{j_{12}}\sum_{j_{12}'}\sum_{l}\sum_{l'} {Y_{l'}}^{*}{}_{M-m_1-m_2}(\Theta_o\Phi_o) \\
& \times (j_1 j_2 m_1 m_2 | j_1 j_2 j_{12}\ m_1+m_2)(l j_{12}\ M-m_1-m_2\ \ m_1+m_2 | l j_{12} J M) \\
& \times T_J^{\pm}(\alpha j_{12} l;\alpha' j_{12}' l')(j_1' j_2' m_1' m_2' | j_1' j_2' j_{12}'\ m_1'+m_2') \\
& \times (j_{12}' l'\ m_1'+m_2'\ \ M-m_1'-m_2' | j_{12}' l' J M)\Big\} Y_{l'\ M-m_1'-m_2'}(\hat{R})|^2 d\hat{R}.
\end{aligned} \tag{2.15}
$$

The corresponding integral cross section is given by

$$
\begin{aligned}
\sigma^{\pm}(n_1 n_2 j_1 j_2 \rightarrow n_1' n_2' j_1' j_2') = & \frac{\pi}{(2j_1+1)(2j_2+1)k_\alpha^2}\sum_{J}\sum_{j_{12}}\sum_{j_{12}'}\sum_{l}\sum_{l'} \\
& \times (2J+1)|T_J^{\pm}(\alpha j_{12} l;\alpha' j_{12}' l')|^2.
\end{aligned} \tag{2.16}
$$

We note that Eqs. (2.15) and (2.16) represent cross sections where the final ro-vibrational wave functions of the two molecules have proper exchange symmetry. The use of symmetrized ro-vibrational wave function in the scattered wave is based on the argument that molecules leaving the interaction region will maintain the correct exchange symmetry. This symmetry is not destroyed unless another collision occurs, but we are working in the single collision regime. Note also that Eq. (2.16) is formally identical to the equation used for collisions of distinguishable molecules except that the latter do not carry $\pm$ labels and the former are restricted to rotational quantum numbers in accord with Eq. (2.11).

The present derivation differs from Takayanagi's [10] in a number of places. The asymptotic wave function in the j_1, m_1, j_2, m_2 representation in Eq. (2.1) differs from his expression in the normalization factors for the incoming plane wave, $[2(1+\delta_{n_1 n_2}\delta_{j_1 j_2}\delta_{m_1 m_2})]^{-\frac{1}{2}}$, and the outgoing spherical wave, $[2(1+\delta_{n_1' n_2'}\delta_{j_1' j_2'}\delta_{m_1' m_2'})]^{-\frac{1}{2}}$. Both are absent in his expression. The latter is introduced into Eq. (2.14) so that the ro-vibrational wave functions associated with the outgoing spherical wave are normalized. Finally, Takayanagi used the following expression for the scattered wave to determine the scattering amplitude,

$$
\begin{aligned}
& \sum_{\alpha'}\sum_{m_1'}\sum_{m_2'}\frac{i}{(k_\alpha k_{\alpha'})^{\frac{1}{2}}}\frac{\exp(ik_{\alpha'}R)}{R}\{q(n_1' j_1' m_1' n_2' j_2' m_2'|\hat{R}) \\
& \pm q(n_2' j_2' m_2' n_1' j_1' m_1'|-\hat{R})\}\chi_{n_1' j_1'}(r_1)Y_{j_1' m_1'}(\hat{r}_1)\chi_{n_2' j_2'}(r_2)Y_{j_2' m_2'}(\hat{r}_2)
\end{aligned} \tag{2.17}
$$

Thus Eq. (2.17) adds up the direct and exchange contribution to the scattering amplitude, but the ro-vibrational wave functions of the two molecules in the scattered wave is not symmetrized; whereas Eq. (2.14) maintains the exchange symmetry of the molecular wave functions. Also, the summation over α', m_1', and m_2' are full sums in Eq. (2.17), whereas in Eq. (2.14) they are restricted sums in order not to sum over redundant terms in the close coupling wave function. Based on matching Eq. (2.17) with the scattered wave in the J-representation, Takayanagi obtained

$$\sigma^{\pm}(n_1 n_2 j_1 j_2 \rightarrow n_1' n_2' j_1' j_2') = \frac{\pi}{(2j_1+1)(2j_2+1)k_\alpha^2} \sum_J \sum_{j_{12}} \sum_{j_{12}'} \sum_l \sum_{l'} (2J+1) \\ (1+\delta_{n_1 n_2}\delta_{j_1 j_2})(1+\delta_{n_1' n_2'}\delta_{j_1' j_2'}) |T_J^{\pm}(\alpha j_{12} l; \alpha' j_{12}' l')|^2, \qquad (2.18)$$

which differs from Eq. (2.16) by the factor $(1+\delta_{n_1 n_2}\delta_{j_1 j_2})(1+\delta_{n_1' n_2'}\delta_{j_1' j_2'})$. Arguing that, for initial states $n_1 j_1 = n_2 j_2$, the number of collisions is half the value for the case $n_1 j_1 \neq n_2 j_2$, Takayanagi [16] introduced a symmetry correction factor of $\frac{1}{2}$ to the density used in the calculation of the energy transfer rate when $n_1 j_1 = n_2 j_2$. In the rate expression, this factor of $\frac{1}{2}$ will cancel out $(1+\delta_{n_1 n_2}\delta_{j_1 j_2})$ in his cross section expression. Note that this factor has already been incorporated in our cross section expression, Eq. (2.16), by the requirement that the incoming flux is δ-function normalized.

In their effective potential formulation for the collisions of identical rigid-rotors, Zarur and Rabitz [17] included a factor of $(1+\delta_{j_1' j_2'})^{-1}$ to Takayanagi's rigid rotor cross section to take care of the double counting in the total cross section when the final states are the same. When vibration is included, this factor becomes $(1+\delta_{n_1' n_2'}\delta_{j_1' j_2'})^{-1}$ and cancels out the corresponding factor in Eq. (2.18). If Takayanagi's symmetry factor of $\frac{1}{2}$ in the case $n_1 j_1 = n_2 j_2$, and Zarur and Rabitz's factor of $(1+\delta_{n_1' n_2'}\delta_{j_1' j_2'})^{-1}$ when $n_1' j_1' = n_2' j_2'$ are incorporated into Eq. (2.18), then the difference between Takayanagi's expression and the present result disappears. It should be emphasized that, in using the present expression, there is no need to tamper with the definition of the density, which we believe is a definite advantage in a study, such as the present one, where cross sections for many different types of transitions are involved.

Schaefer and Meyer [18] reported a close coupling calculation for the elastic scattering of para-H_2 ($j_1 = 0, j_2 = 0$) $\rightarrow$ (0,0) and ortho-H_2 (1,1) $\rightarrow$ (1,1). Their expression for the integral cross section differs from Eq. (2.16) by the factor $(1 + \delta_{n_1 n_2}\delta_{n_1' n_2'}\delta_{j_1 j_2}\delta_{j_1' j_2'})$. If Takayanagi's symmetry factor of $\frac{1}{2}$ is incorporated into their cross section expression, it will reduce to our result in Eq. (2.16). Alternatively, in comparison with experimental data, the symmetry factor can be applied to the density. It is not obvious from their paper whether this has been done.

III. RESULTS AND DISCUSSION

The vdA potential was described in Ref. [7]. For use in the molecular scattering calculations the 20 unique angular expansion terms were interpolated from a tabulated radial grid as described in Ref. [8]. All cross section calculations were done with the MOLSCAT [14] computer code, using the HIBRIDON [19] integrator to solve the coupled equations. Integration parameters were chosen to obtain cross sections generally accurate to about 1%. Nitrogen rotational energies were calculated from the rigid rotor formula using a rotation constant of 1.92265 cm^{-1}. Calculations were done for both even and odd exchange symmetries, and cross sections with no exchange symmetry were deduced from the symmetrized T-matrices as described in Section III B. A few test calculations which compared such results with results calculated directly using a distinguishable molecule basis set confirmed the validity of this procedure.

Due to their prohibitive cost, CC calculations were carried out only for (even j, even j) collisions: a 12-level calculation from 22 to 106 cm^{-1} and an 18-level calculation from 113 to 219 cm^{-1}, the term level denoting the pair of quantum numbers (j_1, j_2 for distinguishable molecules and $j_1 \geq j_2$ for identical molecules) ordered by increasing energy. CS cross sections for (even j, even j) and (odd j, odd j) collisions were computed for energies from 22 to 680 cm^{-1}. The N_2 rotor basis set varied from 12-level to 42-level, the highest level included being (18,6) and (17,7), respectively. For (even j, odd j) CS calculations were carried out

at energies from 20 to 620 cm^{-1}, with (16,7) being the highest level included in the basis. To reduce the computational cost, the largest calculations, i.e., the 42-level case for (even j, even j) and the 30- and 38-level cases for (odd j, odd j) were done with total J increasing in steps of three instead of one, and the 65-level case for (even j, odd j) was done with steps of two. Numerical tests showed that, on the average, this interpolation on J introduced errors of 2-3% in cross sections; this error decreased with increasing energy where more J values are required.

Some calculations with increasing basis set size were done to study convergence of cross sections. These suggested that at least four closed levels must be included to obtain results converged to better than 10%. A comparison between the 36-level and 42-level CS calculations for (even j, even j) with even exchange symmetry illustrates this point. At 500 cm^{-1}, there are six and twelve closed levels in the 36-level and 42-level calculations, respectively, and the average deviation between calculated cross sections is 2.5% and the maximum deviation, 22%. At 550 cm^{-1}, the number of closed levels is two and eight, respectively, and the average and maximum deviations are 10% and 502%. At 590 cm^{-1}, the number of closed channels is one and seven, and the average and maximum deviations are 11% and 151%.

The IOS calculations used the same numerical procedures as described in Ref. [8]; however, a program error in the associated Legendre polynomial subroutine in MOLSCAT has been corrected and the present IOS results supercede the data published previously. The fundamental cross sections, $Q(L_1, L_2)$ through $L_1, L_2 = 18$, were obtained by solving the IOS equations and state-to-state cross sections were deduced from scaling relations.

A. Comparison of CC, CS, and IOS cross sections

Because the CS approximation is expected to be more accurate than the IOS approximation at low energies, the CS results are compared with the CC cross sections in this energy region. This furnishes a test of the CS approximation where it is expected to perform least well. In turn, the IOS results are compared with the CS results at the high energy end of

the CS calculations to determine their accuracy.

The comparison between CC and CS cross sections is presented here only for (even j, even j) collisions using identical molecule symmetry with even exchange and for energies up to 219 cm^{-1}, where CC data are available. The results with odd exchange are similar. At 22 cm^{-1}, the lowest energy calculated, the deviation for the only energetically allowed inelastic channel, (0,0) $\rightarrow$ (2,0), is 26%. Between 22 and 106 cm^{-1} the average deviation is 21%, and between 113 and 219 cm^{-1} it is 14%. Thus the CS approximation gives a reasonable representation of the CC results, even in the low energy region. Table I presents a typical example. Here instead of tabulating all transitions starting from the same initial level or ending with the same final level, Table I lists (at two energies, 119 and 219 cm^{-1}) all transitions starting with at least one molecule in the $j = 0$ level and ending with at least one molecule in the $j = 4$ level. Thus it represents part of the input data used in the calculation of the effective excitation rate for the $0 \rightarrow 4$ transition of N_2 upon collision with a bath of N_2 molecules. The largest difference is 35% for the (0,4) $\rightarrow$ (4,4) transition at 119 cm^{-1}. The smallest is $< 0.1\%$ for the (0,4) $\rightarrow$ (4,0) elastic scattering at 219 cm^{-1}. (Because of exchange symmetry, (0,4) and (4,0) denote the same level.) Elastic cross sections in the CS approximation are consistently in good agreement with the CC results. However, unlike the IOS result discussed in the following paragraph, the difference between CC and CS inelastic cross sections does not seem to correlate with the amount of inelasticity. The next to last entry in Table I presents the sum of all cross sections in the table, including the elastic case, and the last entry presents the sum of all inelastic cross sections. Due to the good agreement between the elastic cross sections and the fact that they are by far the largest, good agreement is found between the two results for the first sum. The second sum roughly represents the contribution to the rate constant at those two energies; a weighed sum instead of direct sum is used in the rate constant calculation. Here a 17.5% difference is found at 119 cm^{-1}, and 13% at 219 cm^{-1}. Based on these results and the fact that the performance of the CS approximation is expected to continue improving as the energy increases, it is concluded that the error introduced in the room temperature excitation rates by the use of

the CS approximation is less than 15%.

At the high energy end of the CS calculation, the validity of the IOS result is tested by comparison with the CS cross sections (for distinguishable molecules). Fig. 1 presents the percent difference between the two sets of cross sections at 680 cm^{-1}; note that this is the relative kinetic energy for the IOS cross sections, but the total energy for the CS cross sections. Again the initial and final levels in the figures are chosen such that at least one molecule initially is in the $j = 0$ level, and at least one molecule is in $j = 4$ after the collision. The known IOS behavior of larger error with increasing inelasticity can be recognized. It is seen from Fig. 1, where entries at the right-most point of the abscissa represent transitions to the (4,16) level, the difference is consistently larger than 100% for initial levels with low (j_1, j_2). Only for initial levels (0,12) and (0,14) is the difference less than 100%. The corresponding results at 500 cm^{-1} have a larger scatter, as expected; the IOS approximation is generally less good at lower collision energies because the inelasticity is then a larger fraction of the collision energy. However, the IOS approximation appears to perform better for the sum of the inelastic cross sections than for individual values. At 680 cm^{-1}, the difference in the sum is 32%, and at 500 cm^{-1} it is 30%. While significant errors are involved in the IOS cross sections, it has been shown in Ref. [8] that methods which enforce detailed balance and which correct for effects of inelasticity improve the IOS results. None of these corrections have been used here; however, they will be discussed and applied to the rate constants which are presented in Sec. III C.

B. The Role of Exchange Symmetry

Exchange symmetry of identical molecules is a purely quantum mechanical phenomenon. Because classical mechanics is frequently used to study molecule-molecule collisions and also because all previous quantal treatments of this system consistently neglected exchange symmetry, it is of some interest to determine its importance for this system.

A basic assumption underlying the discussion of identical molecule symmetry is that ther-

mal energy nonreactive collisions do not change the *nuclear* spin states, I_i, of the molecules. Molecules which differ in their nuclear spin states can, in principle, be identified after the collision and thus are described by distinguishable molecule collision dynamics. For collisions of identical molecules ($I_1 = I_2 = I$) the *total* scattering wave function must be either symmetric or anti-symmetric with respect to exchange of the two molecules, depending on whether I is an integer (Bose-Einstein statistics) or a half-odd integer (Fermi-Dirac statistics). Eq. (2.3) defines symmetrized VRT scattering basis for the spatial coordinates, and these must be combined with total nuclear spin functions of the appropriate symmetry (cf. Ref. [10]). The total nuclear spin functions, I_{tot}, are the vector sum of I_1 and I_2 and it turns out that for $I_{tot} = 2I, 2I-2, \ldots, 0$ the spin wave functions are symmetric and for $I_{tot} = 2I-1, \ldots, 1$ they are anti-symmetric. [20] For a homonuclear molecule like N_2, similar considerations applied to the individual nuclei require that even rotational levels, which are symmetric, combine only with symmetric N_2 spin functions ($I = 0, 2$) and odd rotational levels, which are anti-symmetric, combine only with anti-symmetric spin functions ($I = 1$). In an experiment which does not distinguish nuclear hyperfine structure, the measured cross sections for identical particles are obtained from

$$\sigma(j_1 j_2 \rightarrow j_1' j_2') = w^+ \sigma^+(j_1 j_2 \rightarrow j_1' j_2') + w^- \sigma^-(j_1 j_2 \rightarrow j_1' j_2') \,, \tag{3.1}$$

where w^+ is the fraction of the $(2I+1)^2$ total nuclear spin states associated with even exchange symmetry and w^- that associated with odd exchange; the weights depend on the nuclear spin, I, and whether the nuclei involved obey Bose-Einstein or Fermi-Dirac statistics. [10] The $\sigma^{\pm}$ are obtained from Eq. (2.16).

The expansion basis set for the spatial coordinates of identical molecules, Eqs. (2.1) and (2.3), is a linear combination of the basis set used for distinguishable molecules. Since it is assumed that T-matrix elements are diagonal in the nuclear spin functions, one can readily transformed from one basis to the other, providing relationships among identical and distinguishable molecule cross sections. In particular, Eq. (2.3) shows that properly symmetrized basis functions for identical molecules can be written in terms of those for

distinguishable molecules (see also Ref. [21]). The cross section expression for identical rigid rotors is obtained by rewriting Eq. (2.16) as

$$\sigma^{\pm}(j_1 j_2 \to j_1' j_2') = \sum_{J j_{12} j_{12}' l l'} B_J \, |T_J^{\pm}(j_1 j_2 j_{12} l; j_1' j_2' j_{12}' l')|^2 \tag{3.2}$$

where

$$B_J = \frac{(2J+1)\pi}{(2j_1+1)(2j_2+1)k_\alpha^2} \, .$$

Using Eq. (2.3) the T-matrices in the identical molecule basis can be readily expressed in terms of T-matrix elements in a distinguishable molecule basis as

$$T_J^{\pm}(j_1 j_2 j_{12} l; j_1' j_2' j_{12}' l') = 2\mathcal{N}\mathcal{N}' \left[T_J(j_1 j_2 j_{12} l; j_1' j_2' j_{12}' l') \pm \mathcal{P}' T_J(j_1 j_2 j_{12} l; j_2' j_1' j_{12}' l') \right] , \tag{3.3}$$

where the normalization and the parity factors are

$$\mathcal{N} = [2(1+\delta_{j_1 j_2})]^{-\frac{1}{2}},$$

$$\mathcal{P}' = (-1)^{j_1'+j_2'+j_{12}'+l'} .$$

It should be recalled that symmetrized quantities (indicated by a $\pm$ superscript) are limited to "well-ordered" sets of rotational states, for example, $j_1 \geq j_2$. Substituting into Eq. (3.2), the identical molecule cross sections can be written as

$$\sigma^{\pm}(j_1 j_2 \to j_1' j_2') = \sigma^d + \sigma^{ex} \pm \xi \, , \tag{3.4}$$

where

$$\sigma^d(j_1 j_2 \to j_1' j_2') = 4\mathcal{N}^2\mathcal{N}'^2 \sum_{J j_{12} j_{12}' l l'} B_J \, |T_J(j_1 j_2 j_{12} l; j_1' j_2' j_{12}' l')|^2 \, , \tag{3.5}$$

$$\sigma^{ex}(j_1 j_2 \to j_1' j_2') = 4\mathcal{N}^2\mathcal{N}'^2 \sum_{J j_{12} j_{12}' l l'} B_J \, |T_J(j_1 j_2 j_{12} l; j_2' j_1' j_{12}' l')|^2 \, , \tag{3.6}$$

and

$$\xi(j_1 j_2 \to j_1' j_2') = 4\mathcal{N}^2\mathcal{N}'^2 \sum_{J j_{12} j_{12}' l l'} 2 \, B_J \, \mathcal{P}' \, Re \, \{ T_J(j_1 j_2 j_{12} l; j_1' j_2' j_{12}' l') T_J(j_1 j_2 j_{12} l; j_2' j_1' j_{12}' l')^* \} . \tag{3.7}$$

The first two terms in Eq. (3.4) give cross sections which would have been obtained in calculations for distinguishable molecules. The first,

$$\sigma^d(j_1 j_2 \to j_1' j_2') = (1+\delta_{j_1 j_2})^{-1}(1+\delta_{j_1' j_2'})^{-1}\sigma(j_1 j_2 \to j_1' j_2')\,, \tag{3.8}$$

we call the direct cross section, and the second,

$$\sigma^{ex}(j_1 j_2 \to j_1' j_2') = (1+\delta_{j_1 j_2})^{-1}(1+\delta_{j_1' j_2'})^{-1}\sigma(j_1 j_2 \to j_2' j_1')\,, \tag{3.9}$$

we call the exchange cross section since it exchanges the role of j_1' and j_2'. Recall that σ^d and σ^{ex}, as derived from Eq. (3.4) are defined only for "well-ordered" rotor levels whereas the labeling for the distinguishable cross section σ on the right-hand-side of Eqs. (3.8) and (3.9) need not be well-ordered. The third term in Eq. (3.4) is a cross term; unlike σ^d and σ^{ex}, which are nonnegative, ξ can be of either sign. It is this term which contains the quantum interference effects. It is obvious from Eq. (3.4) that the importance of quantum interference effects is measured by the difference between σ^+ and σ^-.

Just as indistinguishable molecule cross sections can be written in terms of distinguishable molecule T-matrices and hence related to distinguishable molecule cross sections, conversely, distinguishable molecule cross section can also be obtained from T-matrices in an identical molecule basis. In fact, for coupled channel methods the latter are less expensive to obtain computationally and so calculations are generally done in the identical molecule basis, a procedure used in the present study. Distinguishable molecule cross sections are then obtained from

$$\begin{aligned}\sigma(j_1 j_2 \to j_1' j_2') = {} & \frac{1}{2}(1+\delta_{j_1 j_2})(1+\delta_{j_1' j_2'}) \\ & \times \left[\sigma^+(\overline{j_1 j_2} \to \overline{j_1' j_2'}) + \sigma^-(\overline{j_1 j_2} \to \overline{j_1' j_2'}) + \mathcal{Q}\mathcal{Q}'\,\xi^{\pm}(\overline{j_1 j_2} \to \overline{j_1' j_2'})\right]\,,\end{aligned} \tag{3.10}$$

where $\overline{j_1 j_2}$ indicates a possible reordering to give $j_1 \geq j_2$ as required for the identical particle basis set, and the sign change which may be necessitated by this reordering is given by

$$\mathcal{Q} = \begin{cases} +1, & j_1 \geq j_2 \\ -1, & j_1 < j_2 \end{cases}\,.$$

The cross term in the identical molecule basis, $\xi^{\pm}$, is given by

$$\xi^{\pm}(\overline{j_1 j_2} \rightarrow \overline{j_1' j_2'}) = \sum_{J j_{12} j_{12}' l l'} 2\, B_J\, Re\, \left\{ T_J^{+}(\overline{j_1 j_2} j_{12} l; \overline{j_1' j_2'} j_{12}' l')\; T_J^{-}(\overline{j_1 j_2} j_{12} l; \overline{j_1' j_2'} j_{12}' l')^{*} \right\} . \quad (3.11)$$

Finally, it should be noted that even though Eqs. (3.2) – (3.11) are expressed within the CC formalism, exactly analogous results hold for the CS approximation as well.

A comparison of σ^{+} and σ^{-} (referred to below as even and odd cross sections) calculated in the present work showed that the two sets of results are very close. Fig. 2 presents the difference between σ^{+} and σ^{-} from the lowest eight initial levels to the lowest 14 final levels at 219 cm^{-1}. The largest difference was only 6% [for (6,2) $\rightarrow$ (0,0)] with an average difference of only 1%. At a total energy of 113 cm^{-1} the largest difference in CC cross sections was 19% [for the transition (6,0) $\rightarrow$ (0,0)] and the average difference was 3%. The improved agreement with increasing energy, indicated by the CC data at 113 and 219 cm^{-1}, continued at higher energies. In the energy range 500–600 cm^{-1}, the average difference between the CS even and odd cross sections was only 0.5%. From Eq. (3.4) the close agreement between σ^{+} and σ^{-} indicates a near zero cross term, ξ. Table II shows the even and odd cross sections as well as σ^{d} and σ^{ex} for a number of state-to-state transitions at several energies. When the quantum exchange effects average to zero, as we find here,

$$\sigma \approx \sigma^{+} \approx \sigma^{-} \approx \sigma^{d} + \sigma^{ex}$$

since the spin statistics weights in Eq. (3.1) add to one. The fact that indistinguishable molecule effects are unimportant here is perhaps not surprising; it is well known, for example, that such effects are not important for gas kinetic properties of moderately heavy particles at thermal energies. [22]

The near vanishing of the cross term could signify that all the terms in the partial wave (J) sum in Eq. (3.7) are small or it could signify cancellation of different terms. Fig. 3 presents the difference between the partial cross sections σ_J^{+} and σ_J^{-} as a function of J for the (2,0) $\rightarrow$ (6,4) transition at 219 and 680 cm^{-1}. The partial cross sections are defined in an obvious way from Eq. (3.2) as

$$\sigma_J^{\pm} = \frac{\pi}{(2j_1+1)(2j_2+1)k_\alpha^2} \sum_{j_{12}} \sum_{j'_{12}} \sum_{l} \sum_{l'} (2J+1) |T_J^{\pm}(j_1 j_2 j_{12} l; j'_1 j'_2 j'_{12} l')|^2, \tag{3.12}$$

so that $\sigma^{\pm} = \sum_J \sigma_J^{\pm}$. It is clear from Fig. 3 that the difference between individual $\sigma_J^{\pm}$ can be large, but that the oscillatory structure leads to nearly complete cancellation on summing over J. Indeed, it is quite impressive that, in spite of the large oscillations, the differences between σ^+ and σ^- for this transition are only 0.3% and 0.03% at 219 and 680 cm^{-1}, respectively.

The fact that the cross term, ξ, is nearly zero, so that

$$\sigma^{\pm}(j_1 j_2 \rightarrow j'_1 j'_2) \approx \sigma^d(j_1 j_2 \rightarrow j'_1 j'_2) + \sigma^{ex}(j_1 j_2 \rightarrow j'_1 j'_2), \tag{3.13}$$

represents a necessary condition for a classical treatment to be applicable, provided exchange is accounted for by adding the exchange cross section to the direct term. On the other hand, the large deviations between σ_J^+ and σ_J^- indicate that at a detailed level the system is still quantal, not classical. Effects of this quantum behavior might be observable, for example, in differential cross sections. Even at the highest energy used in the CS calculation, 680 cm^{-1}, σ_J^+ and σ_J^- still behave quantally. Only in a global sense, upon summation over J, does the system exhibit classical behavior.

In a seminal paper, Gioumousis and Curtiss [12] suggested that at the classical limit, the cross terms would be rapidly varying functions with a mean value of zero and so might be ignored. Our results support the accuracy of this "random phase approximation" for the total cross section $\sigma^{\pm}$ in thermal N_2 collisions. The fact that more partial waves contribute to the cross section at higher energies is consistent with greater cancellation leading to the smaller differences between σ^+ and σ^- found at higher energies.

C. Rotational Excitation Rate Constants

A thermal velocity average of the state-to-state cross sections, $\sigma(j_1 j_2 \rightarrow j'_1 j'_2)$, gives the two-body rotational excitation rates for the rigid rotors, $R(j_1 j_2 \rightarrow j'_1 j'_2)$. Experiments often measure an effective one-particle excitation rate, the case of a "test particle" in a thermal

bath, which is obtained by averaging over a thermal distribution of the initial bath states and summing over the final bath states. If the bath is composed of molecules which are distinguishable from the "test particle," the effective one-body rotational excitation rate constants $\mathcal{R}(j_1 \to j_1')$ are given by

$$\mathcal{R}(j_1 \to j_1') = \sum_{j_2 j_2'} \rho(j_2) R(j_1 j_2 \to j_1' j_2'), \tag{3.14}$$

where $\rho(j_2)$ is the distribution of initial bath states. This distribution is given by

$$\rho(j_2) = (2j_2 + 1) g_{j_2} e^{-E_{j_2}/kT} / \sum_j (2j + 1) g_j e^{-E_j/kT} \tag{3.15}$$

where k is the Boltzmann constant, T is the temperature, and the nuclear spin statistics degeneracies for N_2 are $g_j = 1$ for odd j and $g_j = 2$ for even j. This procedure is obvious for excitation by a bath of foreign molecules, for example, excitation of N_2 by H_2; but it applies equally to excitation of N_2 by N_2 molecules which are distinguishable because they have different nuclear spin, i.e., $I_2 \neq I_1$.

In the following, distinguishable rates for the N_2-N_2 case are considered first, followed by a discussion of identical molecule rates. We argue here that experiments such as Sitz and Farrow's, [2] which measure the rotational excitation of N_2 in the $n = 1$ level by a bath of molecules in the ground vibrational level, measure essentially distinguishable molecule rates. At thermal energies vibrational excitation is very much slower than rotational excitation and it is believed that pure rotational excitation rates for this system depend only weakly on the vibrational level. This corresponds to intermolecular potential coupling matrix elements which are nearly independent of and diagonal in vibrational level, an approximation which has been useful for this and similar systems. In the limit of zero vibrational coupling it is readily shown that the two vibrational states can be treated formally as distinguishable molecules. Based on these considerations, rotational excitation of N_2 due to collisions with a bath of N_2 molecules in a different vibrational level may be treated using distinguishable molecule rates.

The one- and two-body rates evaluated using available CC plus CS cross sections are referred to below as coupled channel rates and labeled as CC-CS. In evaluating Eq. (3.14)

it is necessary to include all the significantly populated bath levels, j_2. At 300 K the distribution among even rotational levels peaks at $j \approx 6$–8, and including levels through $j = 18$ recovers about 97% of the population. While $j = 18$ was the highest rotational level we were able to include in our CS calculations it was not possible to include basis functions where both rotors reached this value. In fact, $j = 16$ was the highest level for which we obtained adequate cross sections for a thermal average to get rate constants. It is therefore desirable to extrapolate the coupled channel results somewhat to obtain effective one-body thermal rates; such extrapolations will be even more important when considering rates at elevated temperatures. We considered several extrapolation schemes based on the IOS and ECS scaling laws. [8]

Both IOS and ECS provide a prescription for obtaining all the state-to-state rates, $R(j_1 j_2 \rightarrow j_1' j_2')$, from a limited subset of "fundamental" rates, $Q(L_1, L_2)$, using the scaling relationship:

$$R(j_1 j_2 \rightarrow j_1' j_2') = (2j_1' + 1)(2j_2' + 1) \times \sum_{L_1 L_2} D(j_1 j_2, L_1 L_2)^2 \begin{pmatrix} j_1 & L_1 & j_1' \\ 0 & 0 & 0 \end{pmatrix}^2 \begin{pmatrix} j_2 & L_2 & j_2' \\ 0 & 0 & 0 \end{pmatrix}^2 Q(L_1 L_2)\,, \qquad (3.16)$$

where (:::) is a $3j$-symbol. Eq. (3.16) is applied only to energetically downward collisions, those in which energy is transferred from rotational to translational degrees of freedom. Upward rates are obtained from the corresponding downward rates using the detailed balance requirement. The ECS correction factor, introduced by DePristo, et al., [23] is given by

$$D(j_1 j_2, L_1 L_2) = \frac{\{6 + [\alpha l_c (\mu/T)^{\frac{1}{2}} \Omega(L_1 L_2)]^2\}}{\{6 + [\alpha l_c (\mu/T)^{\frac{1}{2}} \Omega(j_1 j_2)]^2\}}\,. \qquad (3.17)$$

Here μ is the reduced mass of the colliding system, l_c a "critical impact parameter," T the temperature; and α is a proportionality constant with a value of 0.065 for l_c in Å, reduced mass in atomic mass units, temperature in K, and Ω in cm^{-1}. The frequency factor, $\Omega(j_1 j_2)$, representing the energy spacing between rotational levels, can be chosen in various ways. [8] In the present work we used $\Omega(j_1 j_2) = 2B_e(j_1 + j_2)$ where B_e is the N_2

rotational constant; this was found in Ref. [8] to give the most reasonable results. For pure IOS scaling, $l_c = 0$ so that $D(j_1 j_2, L_1 L_2) = 1$. It should be noted that this scaling relation applies to distinguishable molecules; although IOS may be applied to identical molecules, cross terms arise which appear to preclude such simple scaling laws.

A variety of methods for extrapolating the coupled channel results can be obtained within this IOS/ECS scaling framework by using different choices for the "fundamental" rates. We describe here methods which appeared to be reasonable as judged from their ability to reproduce the calculated coupled channel values. The first simply takes the fundamental rates from the coupled channel values for $R(0,0 \rightarrow L_1, L_2)$:

$$\begin{aligned} Q(L_1, L_2) &= [(2L_1+1)(2L_2+1)]^{-1} R(L_1, L_2 \rightarrow 0, 0) \\ &= e^{(E_{L_1}+E_{L_2})/kT} R(0,0 \rightarrow L_1, L_2)\,. \end{aligned} \tag{3.18}$$

These were available only through $L_1, L_2 = 16, 4$, and also excluded $14,10$, $14,12$, and $14,14$. However, it was possible to obtain all fundamentals to $L_1, L_2 = 16, 16$ by using

$$Q(L_1, L_2) = (2L_1+1)^{-1} R(0, L_1 \rightarrow L_2, 0),\ L_1 \geq L_2 \tag{3.19}$$

for those which could not be obtained via Eq. (3.18). By comparing IOS/ECS scaling predictions with the 4901 coupled channel values it was found that ECS corrections, i.e., nonzero l_c in Eq. (3.17), did not improve on pure IOS scaling. The median absolute relative error from the IOS scaling using these base rates was 17.5%, with an average of 87%; only 16% of the predicted rates were in error by more than a factor of two and 28% by more than 50%. The much larger root mean square relative error of 352% is heavily weighted by a small number of very poor predictions. This extrapolation scheme is designated here as CSX and the fundamental rates are listed in Table III.

It should be realized that the CSX fundamentals could have been obtained exclusively from Eq. (3.19). If the scaling method were exact this would give the same rates as Eq. (3.18). We have examined this by using the fundamentals deduced from $R(0,0 \rightarrow j_1, j_2)$ via Eq. (3.18) to predict $R(0, j_1 \rightarrow j_2, 0)$; for $j_1, j_2 \leq 12$ the relative errors were typically less

than 20% and almost always less than 50%, consistent with the overall accuracy of the fit. As might be expected there was a trend for increasing discrepancy with increasing difference in the inelasticity of the two rates.

The second method determines the fundamental rates via a weighted linear least-squares fit of Eq. (3.16) to the complete set of 4901 coupled channel values. This has the potential advantage of allowing the determination of fundamental rates for $L_1, L_2 > 16$. [Note that the limit on the sum in Eq. (3.16) is determined by the 3-j symbols and includes values as high as the highest $j_1 + j_1'$; these are set to zero if not available.] In practice, however, it was found that using $L_{max} > 16$ resulted in negative values for fundamental rates which, of course, is disallowed. The nonlinear l_c parameter was varied manually for each L_{max}. The best fit was found with $L_{max} = 16$ and $l_c = 2.5$. It should be noted that $l_c = 2.5$ gave the best fit by all criteria considered, but variation with l_c was not dramatic; for example, the root mean square relative error from the best fit was 49% whereas it was 53% with $l_c = 0$. The median absolute relative error from this scaling method was 34% with an average of 38%; less than 2% of the predicted rates were in error by more than a factor of two and only 29% were in error by more than 50%. The much lower root mean square relative error found here can be attributed to the fact that this quantity is minimized by the fit. This extrapolation scheme is designated here as LSQ and the fundamental rates are listed in Table III.

The third method is not an extrapolation, but used ab initio IOS values, which were obtained up to $L_{max} = 18$. These were modified as suggested by Chapman and Green [24] and Agg and Clary [5] to partially account for the neglect of inelasticity in the IOS method. It was found that ECS corrections did not improve on IOS scaling when using these ab initio IOS fundamental rates. The median error from this scaling method was 32% with 27% of the rates in error by more than a factor of two and 40% in error by more than 50%. However, the average absolute error and rms relative error from this method were extremely large owing to extremely large errors in a small fraction of the rates (mainly those with large inelasticity). This method is designated here as IOS and the fundamental rates are listed in

Table III.

The rates presented in Table III and in subsequent tables are given in units of $\mu\text{sec}^{-1}\text{torr}^{-1}$ which are not standard units for collision rates but which were chosen to compare more directly with experimental values of Sitz and Farrow. [2] These authors used units more appropriate to a linewidth parameter, and, in particular, reported values corresponding to halfwidth at half maximum for a Lorentzian line profile. A halfwidth in $\mu\text{sec}^{-1}\text{torr}^{-1}$ can be converted to the perhaps more familiar pressure broadening units of 10^{-2} $\text{cm}^{-1}\text{atm}^{-1}$ by dividing by 2.4785 (as noted by Sitz and Farrow). Conversion to more conventional units for collision rates may be effected by noting that 1 $\mu\text{sec}^{-1}\text{torr}^{-1}$ corresponds to 3.0825×10^{-11} $\text{cm}^3\text{sec}^{-1}$.

Effective one-body excitation rates for distinguishable molecules calculated in several ways from Eq. (3.14) are reported in Table IV for even j. The results labeled CC-CS used only thermal averages of the available CC and CS cross sections, preferring CC values when they were available, and setting all missing rates to zero. The sum over j_2 in Eq. (3.14) and in the calculation of the partition function, i.e., the denominator of Eq. (3.15), employed only rotational levels for which cross sections are available. For the CC-CS rates, this means values only through $j_2 = 16$. Note that the effective partition function so determined differs somewhat from its true value; the use of this effective partition function partially compensates for the incompleteness in the set of cross sections used in the rate calculation. Next, these CC-CS rates were supplemented by using the three scaling procedures, CSX, LSQ, and IOS, to obtain the missing values. Here the sum over j_2 included values through $j_2 = 18$, and the sum over j_2' included values through $j_2' = j_2 + 18$. Including extrapolated values is expected to increase the rates because it incorporates the contributions for higher j_2'. While this is generally the behavior found, for some of the lower j_1, j_1' where most of the important rates are included in the CC-CS results, the use of the more complete partition function in the calculation of the CSX, LSQ, and IOS scaled rates leads to a slight decrease when compared with the CC-CS rates. To provide another measure of the accuracy of the scaling methods we have also listed effective one-body rates obtained by calculating *all* of

the two-body rates from the scaling equations, using the same limits on j_2, j_2' as above. Comparing these with the CC-CS plus scaling results, it is seen that the scaling methods are accurate to typically 10–20% for these highly averaged quantities, although accuracy is somewhat less good for the smaller rates.

It should be recalled that the CSX and the IOS schemes differ only in the fundamental base rates which are used: the former are taken from CC-CS calculations and the latter from an ab initio IOS calculation (modified for the ignored energy gaps) and so comparison of these results provides some measure of accuracy of the ab initio IOS. In general, and especially for the larger Δj transitions and for transitions among higher levels, the IOS predictions are overestimates. In this context, we also report in Table IV results obtained directly from ab initio IOS calculations with no corrections for inelasticity and using the IOS scaling relations for both upward and downward collisions (i.e., no detailed balance). These predictions are larger still, suggesting that the correction introduced by Chapman and Green [24] does give improvements but perhaps does not go far enough. The LSQ values are almost always smaller than the CSX values, more so for larger Δj and higher rotor levels; this is most likely attributed to the fact that the former use the ECS correction which tends to reduce rates with larger inelasticity. In general, we believe that the CSX extrapolation is likely to somewhat overestimate rates whereas the LSQ extrapolation is likely to somewhat underestimate them, so that an average might provide the best results. Therefore, distinguishable molecule rates for odd j in Table V are reported for only these two extrapolation schemes in addition to values obtained exclusively from coupled channel results.

The experimental data of Sitz and Farrow [2] are compared in Table IV with the various theoretical results. The CC-CS values augmented with extrapolated CSX and LSQ rates, which we believe to be the most accurate, generally agree with experiment to within experimental error as shown in Fig. 4. The large Δj transitions are exceptions. They are consistently smaller than experiment. This is reasonable in view of the fact that the present calculations neglect exchange, and the additivity of the direct and exchange cross sections

means that the calculated values should approach experiment from below. Even though the preceding paragraphs argue that exchange contribution in the collision between $n = 1$ and $n = 0$ molecules should be significantly smaller than between two molecules in $n = 0$, it is not exactly zero. For large Δj transitions, the direct rate itself is exceedingly small, so exchange may be more important there. The $0 \rightarrow 8$ transition is another example of large discrepancy, $\approx 40\%$, between theory and experiment although there are large uncertainties on the experimental value. The fact that theory is too large is particularly puzzling in light of the preceding argument about exchange contributions.

Part of the discrepancy between theory and experiment may also be due to inaccuracy in the potential. The classical trajectory calculation of Heck and Dickinson [9] indicated some deficiency of the vDA potential which shows up in low energy collisions. Comparing theoretical low-temperature Raman linewidths with SRS data [3] also indicates that the vdA potential may be too attractive in the van der Waals region. While such problems may become less important at higher temperatures, it still may account for some of the discrepancies between theory and experiment.

In the case of identical molecules, the definition of $\mathcal{R}(j_1 \rightarrow j_1')$ needs to be modified. While the two-body rate for identical molecules is a straightforward extension of the corresponding distinguishable molecule rate obtained by thermally averaging the identical molecule cross sections, the meaning of an effective one-body rate for identical molecules is rather obscure. When the molecules are indistinguishable, it is not meaningful to discuss a rate where the initial state of molecule 1 is j_1 and its final state is j_1'. An experimentally meaningful quantity appears to be a rotational relaxation time, for example, the time required for a system of N_2 molecules originally in thermal equilibrium to equilibrate after the addition of a N_2 molecule prepared in a specific j_1 level. The rotational relaxation time of identical molecules can be formally defined in terms of a set of effective one-body rates $\mathcal{R}(j_1 \rightarrow j_1')$. In this sense, it is still meaningful to reduce the large number of two-body cross sections into effective one-body rates, even though the individual one-body rates may not be experimentally measurable.

Although different experiments may require somewhat different definitions of an identical molecule effective one-body relaxation rate, we discuss here only a particular extension of Eq. (3.14) which is derived in the Appendix. Since exchange scattering is allowed only if the rotational levels have the same parity and are associated with the same nuclear spin, the contributions from even and odd j_2 are counted differently. Thus, for excitation of a molecule with even j_1 and nuclear spin I_1,

$$\mathcal{R}_{I_1}(j_1 \to j_1') = \rho(I_1)\mathcal{R}_{I_1}^{\pm}(j_1 \to j_1') + \sum_{\substack{j_2 j_2' \in \text{even} \\ I_2 \neq I_1}} \rho(I_2)\rho(j_2) R(j_1 j_2 \to j_1' j_2') + \sum_{j_2 j_2' \in \text{odd}} \rho(j_2) R(j_1 j_2 \to j_1' j_2') \,. \quad (3.20)$$

The first term on the right-hand-side is the effective one-body rate for identical molecules (with nuclear spin I_1) which is derived in the Appendix; $\rho(I_1)$ is the fractional density of even j molecules with nuclear spin I_1. The second term sums over contributions from (even j, even j) collisions when the two molecules have different nuclear spins and thus are considered distinguishable molecules. For N_2 molecules with even j, the nuclear spin can be either 0 or 2; this term represents the contribution when one molecule has I=0 and the other I=2. The third term represents (even j, odd j) collisions. The two-body rates $R(j_1 j_2 \to j_1' j_2')$ in the second and third terms are distinguishable molecule rates; see Eq. (3.14). A corresponding expression applies to odd j_1, with the "even" and "odd" labels interchanged in Eq. (3.20). However, for N_2 with odd j, the nuclear spin can only be 1, so that the second term in Eq. (3.20) is missing.

Using Eq. (3.20), the effective one-body rate for identical molecule collisions can be readily determined from CC and CS cross sections. For the IOS/ECS results, which were determined without exchange symmetry, excitation rates for identical molecules were calculated using the σ^+ and σ^- generated by Eq. (3.13). The results are presented in Tables VI and VII. The general trends of the identical molecule rates are similar to the distinguishable rates, with the exception that the identical molecules rates for large Δj are significantly larger than the corresponding distinguishable rates, a result of the more prominent role of

exchange contributions when the direct term becomes small.

IV. SUMMARY

Using the interaction potential of van der Avoird, et al., [7] we have computed close coupling cross sections for rotational excitation in N_2-N_2 collisions to total energies corresponding to about 300 K. It is found that several (typically 4–8) energetically closed levels are required to obtain reasonably converged (10%) cross sections. Such calculations tax the limits of currently available computational facilities but are required to provide benchmarks for approximate methods. These results have been extended to total energies of about 1000 K by using the coupled states approximation — again this is near the limit of current computational abilities. The expense of coupled channel methods increases dramatically as more rotational levels become energetically accessible; this is exacerbated in collisions of two rotors where the number of channels is the product of the number of channels for each rotor. It appears from comparisons with the close coupling results that the CS approximation is accurate to 10–20% below 300 K with accuracy appearing to improve with increasing energy as expected. The IOS approximation, which is significantly less expensive than the coupled channel methods is found to be of only moderate accuracy for predicting detailed state-to-state cross sections; not unexpectedly, it is less accurate for highly inelastic transitions. Various methods have been proposed to improve IOS accuracy by approximately correcting for inelasticity; these are more readily applied to thermally averaged rate constants and we have considered a few possibilities within the IOS/ECS scaling formalism. These were reasonably successful, at least for predicting the highly averaged effective one-body excitation rates, and especially if the fundamental rates were obtained from coupled channel results, suggesting the utility of such methods for fitting and extrapolating experimental data. It should be noted that the coupled channel calculations here, although at the limit of current computational feasibility, are barely adequate to provide values needed for a room temperature thermal average and so extrapolation methods such as those employed here are likely

to be important. In this context the CSX extrapolation method might prove particularly useful as CS calculations are required only for the base rates $R(0,0 \rightarrow j_1, j_2)$, a much less expensive undertaking than calculations for the whole matrix of state-to-state rates. This was, in fact, found to be the case in extending the present study to consider Raman spectral linewidths for which data are available to much higher rotational levels and to temperatures of 1500 K. [3] That work reports a reinvestigation of the utility of the IOS and the ECS approximations and presents an improved methodology. However, these modifications have only a small effect for the rotational levels and temperature considered here.

Within the coupled channel frameworks we have considered the effects of identical molecule exchange symmetry which has been ignored in previous studies of this system. First, we note that conflicting formulas for normalizing identical molecule cross sections are found in the literature and we rederive this formula in some detail, finding a difference with the commonly used method of Takayanagi. [10] Second, we find that the quantum interference terms very nearly (within a percent or two) average to zero for integral state-to-state cross sections; that is, to a good approximation the system can be described "classically" with the effect of exchange symmetry taken into account by adding "direct" and "exchange" distinguishable molecule cross sections. On the other hand, we find that quantum interference effects are significant for individual partial wave contributions, even at the highest energy considered, suggesting that such effects may be important in quantities such as differential cross sections.

The most detailed experimental values available for this system are the room temperature state-to-state rates measured by Sitz and Farrow [2] for relaxation of vibrationally excited N_2 in a bath of ground vibrational state molecules. We argue that these correspond to distinguishable molecule rates owing to the small probability of vibrational excitation compared with rotational excitation. We have therefore compared these with distinguishable molecule effective one-body rate constants calculated with the coupled channel methods and from the IOS/ECS scaling methods, finding generally very satisfactory agreement (see Table 4). Comparison of theoretical values obtained in this study with CARS linewidth

parameters will be the subject of a subsequent paper. [3]

ACKNOWLEDGMENTS

SG is supported by NASA Headquarters, Office of Space Science and Applications, Astrophysics Division. This project was initiated when WMH was a visitor at the Institute for Theoretical Atomic and Molecular Physics, Harvard-Smithsonian Center for Astrophysics. She thanks Prof. Alex Dalgarno and Dr. Kate Kirby for their hospitality. The large scale computations in this study were made possible through a grant of Cray C90 time from the Numerical Aeronautical Simulation Facility.

APPENDIX

We wish to consider an effective one-body rate of change of population of molecules in level i, dN_i/dt, owing to collisions with a bath. For the case of a "test" molecule in a bath of structureless atoms this is written in an obvious way as

$$dN_i/dt = -N_i \sum_n \overline{R}(i \to n) + \sum_n N_n \overline{R}(n \to i) \qquad \text{(A-1)}$$

where N_i is the number density in level i and $\overline{R}(i \to j)$ is a collision rate, in units of sec^{-1}, and is equal to the usual rate constant in units of $\mathrm{cm}^3\mathrm{sec}^{-1}$ times the number density of the bath in cm^{-3}. Eq. (A-1) is sometimes called a master equation and, if the rate constants are known, can be used to follow changes with time in the distribution of population among the molecular levels. The first sum gives the rate of transfer out of level i to all other levels and the second sum gives the rate of transfer from all other levels into level i. Note that the elastic term, $i = n$, is customarily excluded from the sum. This is actually not required as its contribution would cancel in the incoming and outgoing terms. For a bath of molecules which are different from the "test" molecule this is readily generalized, cf. Eq. (3.14), to give

$$dN_i/dt = -N_i \sum_n \overline{\mathcal{R}}(i \to n) + \sum_n N_n \overline{\mathcal{R}}(n \to i) \tag{A-2}$$

where the effective one-body rate is obtained by averaging over the initial levels of the bath molecules and summing over final levels, cf. Eq. (3.14):

$$\overline{\mathcal{R}}(i \to n) = \sum_{jk} \rho_j \overline{R}(ij \to nk)\,. \tag{A-3}$$

Here ρ_j is the fractional population in the bath molecule levels and, again, $\overline{R}$ indicates that the rate constants have been multiplied by the number density of the bath molecules to give actual rates.

We need to generalize Eq. (A-3) to the case where the bath molecules are identical to the "test" molecule. In this case we can discuss only a pair of levels occupied by two molecules, and we choose to use "well-ordered" indexing such that we count only over levels $i \geq j$. Because of the normalization for the flux established in Section II, the probability of finding the two molecules initially in levels i and j which is consistent with our definition of the state-to-state cross section, Eq. (2.16), is just the product

$$\rho_{ij} = \rho_i \rho_j\,. \tag{A-4}$$

We focus on an effective identical molecule one-body rate, $\overline{\mathcal{R}}^{\pm}(i \to n)$, which is analogous to Eq. (A-3). The problem for identical molecules is the question of how to count contributions when the bath levels are the same as the initial or final levels of interest. In fact, it is not clear that a unique counting method exists as some transitions contribute both forward and backward flux in a given transition and so cancel in the master equation. We have generally attempted here to exclude such "quasi-elastic" rates, an example of which is $R(ij \to ni)$, from the $i \to n$ rate.

We write the effective one-body rate as

$$\overline{\mathcal{R}}^{\pm}(i \to n) = \sum_{jk} \rho_j\, \mathcal{C}(ijnk)\, \overline{R}^{\pm}(\overline{ij} \to \overline{nk})\,, \tag{A-5}$$

where $\overline{R}^{\pm} = w^{+}\overline{R}^{+} + w^{-}\overline{R}^{-}$, and $\overline{R}^{+}$ and $\overline{R}^{-}$ are two-body excitation rates with even and odd exchange symmetry, i.e., thermal averages of σ^{+} and σ^{-} calculated from Eq. (3.1) and

multiplied by the bath number density. Note that the sum over the bath molecules is not restricted but that pairs of indices may need reordering, as indicated by the $\overline{ij}$ notation, to match the indexing for the identical molecule rates. The counting factor, $\mathcal{C}(ijnk)$ embodies the rules for counting specific contributions and it can be calculated from the following set of logical rules:

$$\mathcal{C}(ijnk) = \begin{cases} 0\ ,\ (j = n \bigcap k = i) \\ 0\ ,\ (j \neq i \bigcap k \neq n \bigcap ((j \neq n \bigcap k = i) \bigcup (j = n \bigcap k \neq i))) \\ 2\ ,\ (j = i \bigcap k = n \bigcap i \neq n) \\ 1\ ,\ \text{otherwise} \end{cases} \tag{A-6}$$

Here $a \bigcap b$ indicates *a and b*, i.e., both conditions must be met, and $a \bigcup b$ indicates *a or b*. This counting formula applies only to the inelastic effective one-body rates, $i \neq n$; we assume that elastic effective rates are not included in the master equation. The first rule in Eq. (A-6) excludes the term $R(ij \rightarrow ji)$ which is clearly an elastic term. The second excludes $R(ij \rightarrow ni)$ and $R(in \rightarrow nk)$; we believe that these are more appropriately counted with $\mathcal{R}^{\pm}(j \rightarrow n)$ and $\mathcal{R}^{\pm}(i \rightarrow k)$, respectively, than with $\mathcal{R}^{\pm}(i \rightarrow n)$. The third rule counts $R(ii \rightarrow nn)$ as transferring two molecules per collision.

Using the fact that $\mathcal{C}(ijnk) = \mathcal{C}(nkij)$, which is readily verified, and the detailed balance relation which applies to the two-body rates,

$$\rho_{ij} R^{\pm}(\overline{ij} \rightarrow \overline{nk}) = \rho_{nk} R^{\pm}(\overline{nk} \rightarrow \overline{ij})\,, \tag{A-7}$$

it is readily shown that these effective one-body rates are related by the expected detailed balance relation,

$$\rho_i \overline{\mathcal{R}}^{\pm}(i \rightarrow n) = \rho_n \overline{\mathcal{R}}^{\pm}(n \rightarrow i)\,. \tag{A-8}$$

REFERENCES

[1] C. Park, *Nonequilibrium Hypersonic Aerothermodynamics*, (Wiley, New York, 1990).

[2] G. O. Sitz and R. L. Farrow, J. Chem. Phys. **93**, 7883 (1990).

[3] W. M. Huo and S. Green, J. Chem. Phys., submitted.

[4] M. L. Koszykowski, L. A. Rahn, R. E. Palmer, and M. E. Coltrin, J. Phys. Chem. **91**, 41 (1987).

[5] P. J. Agg and D. Clary, Molec. Phys. **73**, 317 (1991).

[6] G. D. Billing and L. Wang, J. Phys. Chem. **96**, 2572 (1992).

[7] A. van der Avoird, P. E. S. Wormer, and A. P. J. Jansen, J. Chem. Phys. **84**, 1629 (1985).

[8] S. Green, J. Chem. Phys. **98**, 257 (1993); *erratum*, J. Chem. Phys. **99**, 4875 (1993).

[9] E.L. Heck and A. S. Dickinson, Molec. Phys. **81**, 1325 (1994).

[10] K. Takayanagi, Adv. At. Mol. Phys. **1**, 149 (1965).

[11] K. Takayanagi, Progr. Theoret. Phys. (Kyoto) **11**, 557 (1954).

[12] G. Gioumousis and C. F. Curtiss, J. Chem. Phys. **29**, 996 (1958); G. Gioumousis and C. F. Curtiss, J. Math. Phys. **2**, 96 (1961).

[13] W. D. Davison, Disc. Faraday Soc. **33**, 71 (1962).

[14] J. M. Hutson and S. Green, MOLSCAT computer code, distributed by Collaborative Computational Project No. 6 of the Science and Engineering Research Council, UK. The code, documentation, and test cases are available via the Word Wide Web at http://molscat.giss.nasa.gov/MOLSCAT/.

[15] E. U. Condon and G. H. Shortley, *The Theory of Atomic Spectra*, (Cambridge, 1935).

[16] K. Takayanagi, Progr. Theoret. Phys. (Kyoto) Suppl. **25**, 1 (1963).

[17] G. Zarur and H. Rabitz, J. Chem. Phys. **60**, 2057 (1974).

[18] J. Schaefer and W. Meyer, J. Chem. Phys. **70**, 344 (1979).

[19] M. H. Alexander and D. E. Manolopoulos, J. Chem. Phys. **86**, 2044 (1987).

[20] D. Herzberg, *Molecular Spectra and Molecular Structure. I. Spectra of Diatomic Molecules*, 2nd Edition, (Van Nostrand, Princeton, NJ, 1950)

[21] T. G. Heil, S. Green, and D. J. Kouri, J. Chem. Phys. **68**, 2562 (1978).

[22] J. O. Hirschfelder, C. F. Curtiss, and R. B. Bird, *Molecular Theory of Gases and Liquids*, (Wiley, New York, 1964).

[23] A. E. DePristo, S. D. Augustin, R. Ramaswamy, and H. Rabitz, J. Chem. Phys. **71**, 850 (1979).

[24] S. Green and S. Chapman, Chem. Phys. Lett. **98**, 467 (1983); S. Chapman and S. Green, Chem. Phys. Lett. **112**, 436 (1984).

TABLES

TABLE I. Comparison of CC and CS cross sections (in Å^2) at 219 and 119 cm^{-1}

j_1, j_2	j_1', j_2'	CC	CS	% diff	CC	CS	% diff
		E = 119.0 cm^{-1}			E = 219.0 cm^{-1}		
0,0	4,0	2.55	2.09	18.1	1.88	1.27	32.5
0,0	4,2	11.02	7.78	29.5	5.63	4.75	15.7
0,0	4,4	4.98	3.93	21.1	3.60	2.74	23.8
0,0	4,6				3.77	3.32	11.9
0,0	4,8				1.49	1.67	-12.2
0,2	4,0	9.17	12.16	-32.6	6.04	5.20	13.9
0,2	4,2	26.39	19.90	24.6	1.62	1.08	33.5
0,2	4,4	10.00	6.82	31.9	5.79	4.24	26.8
0,2	4,6				7.67	7.07	7.9
0,2	4,8				3.84	4.25	-10.8
0,4	4,0	268.26	277.04	-2.9	259.51	259.56	-0.0
0,4	4,2	34.08	27.84	18.3	18.61	21.90	-17.7
0,4	4,4	12.39	8.06	34.9	6.03	4.36	27.8
0,4	4,6				8.32	8.02	3.6
0,4	4,8				5.95	6.33	-6.4
0,6	4,0	10.04	9.61	4.3	3.72	4.55	-22.5
0,6	4,2	35.59	33.58	5.7	13.14	10.06	23.5
0,6	4,4	23.39	16.38	29.9	5.16	4.99	3.4
0,6	4,6				10.39	8.29	20.3
0,6	4,8				7.59	7.75	-2.1
0,8	4,0				1.58	1.67	-5.7
0,8	4,2				6.33	6.28	0.9
0,8	4,4				6.65	5.89	11.4

0,8	4,6				15.22	12.54	17.6
0,8	4,8				11.77	9.52	19.1
0,10	4,0				2.64	3.29	-24.9
0,10	4,2				7.31	7.83	-7.1
0,10	4,4				9.69	7.12	26.5
0,10	4,6				31.73	21.88	31.0
0,10	4,8				44.98	36.78	18.2
Sum		447.86	425.18	5.1	517.65	484.20	6.5
Sum[a]		179.60	148.14	17.5	258.14	224.64	13.0

[a]The elastic term 0,4 → 4,0 has been omitted from the summation.

TABLE II. Selected cross sections (in Å^2) calculated with even and odd exchange symmetries and with no exchange.

j_1, j_2	j_1', j_2'	$\sigma^+(j_1 j_2 \to j_1' j_2')$	$\sigma^-(j_1 j_2 \to j_1' j_2')$	$\sigma^d(j_1 j_2 \to j_1' j_2')$	$\sigma^{ex}(j_1 j_2 \to j_2' j_1')$	$\sigma^d + \sigma^{ex}$
			E = 680 cm^{-1} [a]			
2,0	6,4	3.44	3.44	1.89	1.55	3.44
	8,4	2.20	2.20	1.12	1.08	2.20
	10,6	1.66	1.66	0.87	0.79	1.66
6,2	6,4	6.24	6.23	4.77	1.47	6.23
	8,4	3.28	3.28	2.26	1.03	3.28
	10,6	2.48	2.48	1.42	1.05	2.48
8,2	6,4	3.96	3.96	2.80	1.15	3.96
	8,4	5.85	5.85	4.99	0.85	5.84
	10,6	2.48	2.48	1.75	0.73	2.48
			E = 500 cm^{-1} [a]			
2,0	6,4	4.13	4.14	2.23	1.90	4.13
	8,4	2.53	2.52	1.30	1.23	2.53
	10,6	1.80	1.80	1.05	0.75	1.80
6,2	6,4	7.03	7.02	5.23	1.80	7.03
	8,4	4.00	4.01	2.80	1.20	4.00
	10,6	2.77	2.77	1.82	0.95	2.77
8,2	6,4	4.83	4.83	3.31	1.52	4.83
	8,4	6.69	6.68	5.66	1.03	6.68
	10,6	2.90	2.90	2.25	0.65	2.90
			E = 369 cm^{-1} [b]			
2,0	6,4	4.98	4.99	2.78	2.21	4.99
	8,4	2.91	2.91	1.64	1.27	2.91
	10,6	1.84	1.85	1.18	0.67	1.85

6,2	6,4	7.89	7.88	5.63	2.26	7.88
	8,4	5.10	5.10	3.75	1.35	5.10
	10,6	2.93	2.93	2.13	0.80	2.93
8,2	6,4	6.30	6.31	4.18	2.13	6.30
	8,4	7.97	7.97	6.69	1.28	7.97
	10,6	3.28	3.29	2.73	0.56	3.29

[a]Calculated in the CS approximation with J steps of 3.

[b]Calculated in the CS approximation with J steps of 1.

TABLE III. Base rates at a temperature of 300 K in $\mu sec^{-1} torr^{-1}$ [a] used in the IOS/ECS extrapolations.

L_1	L_2	CSX	LSQ[b]	IOS[c]
2	0	2.3577	2.1025	1.9909
2	2	5.0115	3.6386	6.3585
4	0	0.5243	0.5368	0.4447
4	2	1.6997	1.4100	1.3924
4	4	1.9743	1.4609	2.2350
6	0	0.3131	0.3534	0.2372
6	2	0.6224	0.5034	0.3938
6	4	1.2074	0.7069	0.9942
6	6	1.3250	0.6309	1.3889
8	0	0.2027	0.1811	0.1186
8	2	0.3120	0.2401	0.2558
8	4	0.5618	0.2951	0.3914
8	6	0.9403	0.3227	0.8601
8	8	0.9828	0.2151	1.0812
10	0	0.0852	0.0438	0.0590
10	2	0.2019	0.0728	0.1776
10	4	0.2023	0.0756	0.2291
10	6	0.4939	0.1005	0.4252
10	8	0.6995	0.0331	0.7547
10	10	0.7281	0.0047	0.8456
12	0	0.0453	0.0093	0.0355
12	2	0.0865	0.0105	0.0999
12	4	0.0892	0.0120	0.1604
12	6	0.1442	0.0170	0.2223

12	8	0.3249	0.0034	0.4078
12	10	0.4650	0.0010	0.6075
12	12	0.1237	0.0002	0.6266
14	0	0.0142	0.0010	0.0212
14	2	0.0207	0.0034	0.0550
14	4	0.0340	0.0029	0.0985
14	6	0.0382	0.0027	0.1354
14	8	0.1514	0.0002	0.2033
14	10	0.0750	0.0002	0.3427
14	12	0.0229	0.0000	0.4581
14	14	0.0088	0.0000	0.4482
16	0	0.0020	0.0001	0.0117
16	2	0.0029	0.0002	0.0318
16	4	0.0110	0.0003	0.0548
16	6	0.0046	0.0001	0.0822
16	8	0.0144	0.0003	0.1094
16	10	0.0113	0.0000	0.1743
16	12	0.0024	0.0000	0.2671
16	14	0.0001	0.0000	0.3307
16	16	0.0024	0.0000	0.3219

[a]Rates in $\mu\text{sec}^{-1}\text{torr}^{-1}$ may be converted to $\text{cm}^3\text{sec}^{-1}$ using the multiplicative factor 3.0825×10^{-11}.

[b]Energy corrected sudden (ECS) scaling with a "critical distance" of $l_c = 2.5$.

[c]IOS scaling used fundamental rates through $L_1, L_2 = 18$, the highest of which are not reported here.

TABLE IV. Distinguishable molecule effective one-body excitation rates in $\mu sec^{-1}torr^{-1}$ [a] for N_2-N_2, even j. Values from coupled channel calculations, with scaling extrapolations for higher rotor levels, and also from the scaling extrapolation alone. The experimental data of Sitz and Farrow[b] are also presented.

		Rate constants (300 K)								
			CC-CS plus scaling			scaling only				
j_1	j_1'	CC-CS[c]	CSX	LSQ	IOS	CSX	LSQ	IOS[d]	IOS[e]	Expt[b]
0	2	7.85	7.96	7.74	7.98	8.44	6.14	8.84	9.87	6.64 ± 1.18
0	4	4.08	4.16	4.05	4.15	4.25	3.82	3.99	4.75	3.76 ± 0.83
0	6	2.54	2.67	2.57	2.66	2.72	2.58	2.44	3.08	2.73 ± 0.61
0	8	1.43	1.55	1.45	1.55	1.66	1.35	1.59	2.14	0.86 ± 0.51
0	10	0.55	0.65	0.56	0.68	0.84	0.35	0.96	1.41	0.64 ± 0.12
0	12	0.15	0.19	0.15	0.24	0.26	0.06	0.51	0.83	0.29 ± 0.06
0	14	0.02	0.04	0.02	0.12	0.05	0.01	0.23	0.44	0.22 ± 0.04
2	4	5.25	5.37	5.20	5.38	6.28	4.70	6.29	7.28	5.13 ± 0.58
2	6	3.00	3.15	3.02	3.14	3.16	2.67	2.94	3.65	2.40 ± 0.44
2	8	1.64	1.77	1.66	1.77	1.82	1.35	1.75	2.34	1.52 ± 0.34
2	10	0.73	0.83	0.74	0.86	0.90	0.51	1.04	1.53	0.97 ± 0.22
2	12	0.22	0.27	0.23	0.32	0.35	0.11	0.56	0.94	0.28 ± 0.14
2	14	0.04	0.07	0.04	0.14	0.08	0.02	0.26	0.52	0.12 ± 0.04
4	6	4.31	4.57	4.31	4.58	5.41	3.53	5.50	6.51	4.70 ± 0.60
4	8	2.23	2.38	2.24	2.39	2.36	1.63	2.36	3.08	2.20 ± 0.40
4	10	1.06	1.18	1.08	1.21	1.16	0.74	1.27	1.88	1.40 ± 0.20
4	12	0.38	0.45	0.39	0.49	0.52	0.26	0.68	1.19	0.54 ± 0.13
4	14	0.09	0.16	0.10	0.22	0.18	0.05	0.33	0.71	0.21 ± 0.04
6	8	3.58	3.95	3.62	3.99	4.67	2.65	4.91	6.05	3.37 ± 0.47

6	10	1.60	1.82	1.64	1.86	1.82	1.11	1.90	2.74	2.22 ± 0.29
6	12	0.66	0.80	0.69	0.83	0.83	0.46	0.93	1.63	0.71 ± 0.14
6	14	0.17	0.31	0.21	0.35	0.34	0.15	0.44	1.01	0.23 ± 0.05
8	10	2.88	3.42	2.96	3.48	4.20	2.09	4.44	5.79	2.52 ± 0.41
8	12	1.10	1.34	1.15	1.37	1.50	0.79	1.54	2.54	1.12 ± 0.22
8	14	0.30	0.56	0.38	0.59	0.63	0.30	0.68	1.49	0.29 ± 0.07
10	12	2.30	3.00	2.43	3.06	3.85	1.66	4.03	5.62	2.68 ± 0.43
10	14	0.58	1.12	0.74	1.14	1.27	0.58	1.29	2.44	1.04 ± 0.13
12	14	1.19	2.70	1.56	2.79	3.55	1.32	3.71	5.53	1.83 ± 0.26

[a]Rates in $\mu\text{sec}^{-1}\text{torr}^{-1}$ may be converted to $\text{cm}^3\text{sec}^{-1}$ using the multiplicative factor 3.0825×10^{-11}.

[b]See Ref. [2].

[c]Uses only the available CC-CS rates; others set to zero.

[d]IOS scaling using correction of Ref. [24] for base rates; scaling for downward rates with reverse rates from detailed balance.

[e]IOS scaling for both upward and downward rates (no detailed balance) and base rates calculated assuming that the energy is the initial energy for upward transitions.

TABLE V. Distinguishable molecule effective one-body excitation rates at a temperature of 300 K in $\mu sec^{-1}torr^{-1}$ [a] for N_2-N_2, odd j. Values from coupled channel calculations plus two different extrapolation schemes for higher rotor states.

j_1	j_1'	CC-CS[b]	plus CSX scaling[c]	plus LSQ scaling[c]
1	3	5.82	5.94	5.76
1	5	3.34	3.50	3.36
1	7	2.04	2.16	2.06
1	9	0.98	1.10	1.09
1	11	0.33	0.40	0.34
1	13	0.07	0.10	0.08
3	5	4.61	4.88	4.62
3	7	2.56	2.69	2.56
3	9	1.27	1.42	1.30
3	11	0.52	0.60	0.53
3	13	0.14	0.19	0.15
5	7	3.88	4.19	3.90
5	9	1.82	2.07	1.87
5	11	0.81	0.95	0.84
5	13	0.25	0.35	0.27
7	9	3.12	3.64	3.21
7	11	1.32	1.53	1.36
7	13	0.51	0.67	0.55
9	11	2.50	3.14	2.62
9	13	0.82	1.18	0.92
11	13	1.93	2.81	2.10

[a]Rates in $\mu sec^{-1}torr^{-1}$ may be converted to cm^3sec^{-1} using the multiplicative factor 3.0825×10^{-11}.

[b]Uses only the available CC-CS rates; others set to zero.

[c]Uses CC-CS rates if available and generates the rest from the indicated extrapolation method.

TABLE VI. Identical molecule effective one-body excitation rates at a temperature of 300 K in $\mu sec^{-1}torr^{-1}$ [a] for N_2-N_2, even j. Values from coupled channel calculations plus two different extrapolation schemes for higher rotor states.

j_1	j_1'	CC-CS[b]	plus CSX scaling[c]	plus LSQ scaling[c]
0	2	7.92	8.00	7.79
0	4	4.39	4.44	4.34
0	6	3.08	3.16	3.06
0	8	2.05	2.14	2.05
0	10	1.18	1.24	1.14
0	12	0.61	0.64	0.59
0	14	0.28	0.34	0.29
2	4	5.18	5.24	5.07
2	6	3.19	3.30	3.17
2	8	2.02	2.11	2.01
2	10	1.16	1.24	1.14
2	12	0.58	0.62	0.56
2	14	0.22	0.31	0.25
4	6	4.22	4.41	4.15
4	8	2.42	2.53	2.39
4	10	1.37	1.48	1.37
4	12	0.69	0.75	0.67
4	14	0.24	0.35	0.26
6	8	3.47	3.83	3.48
6	10	1.77	2.00	1.80
6	12	0.86	1.04	0.90
6	14	0.27	0.54	0.35

8	10	2.82	3.36	2.88
8	12	1.21	1.50	1.27
8	14	0.37	0.77	0.49
10	12	2.26	3.01	2.38
10	14	0.68	1.25	0.85
12	14	1.28	2.67	1.60

[a]Rates in μsec^{-1}torr^{-1} may be converted to cm^{3}sec^{-1} using the multiplicative factor 3.0825×10^{-11}.

[b]Uses only the available CC-CS rates; others set to zero.

[c]Uses CC-CS rates if available and generates the rest from the indicated extrapolation method.

TABLE VII. Identical molecule effective one-body excitation rates at a temperature of 300 K in $\mu sec^{-1} torr^{-1}$ [a] for N_2-N_2, odd j. Values from coupled channel calculations plus two different extrapolation schemes for higher rotor states.

j_1	j_1'	CC-CS[b]	plus CSX scaling[c]	plus LSQ scaling[c]
1	3	5.83	5.87	5.69
1	5	3.48	3.60	3.46
1	7	2.32	2.41	2.31
1	9	1.32	1.46	1.34
1	11	0.65	0.71	0.64
1	13	0.27	0.33	0.29
3	5	4.56	4.76	4.50
3	7	2.68	2.79	2.66
3	9	1.50	1.64	1.51
3	11	0.76	0.84	0.77
3	13	0.31	0.38	0.32
5	7	3.81	4.07	3.77
5	9	1.94	2.17	1.97
5	11	0.99	1.12	1.01
5	13	0.40	0.51	0.42
7	9	3.07	3.57	3.13
7	11	1.44	1.64	1.46
7	13	0.60	0.78	0.65
9	11	2.45	3.09	2.55
9	13	0.88	1.28	0.97
11	13	1.80	2.68	1.95

[a]Rates in $\mu sec^{-1} torr^{-1}$ may be converted to $cm^3 sec^{-1}$ using the multiplicative factor 3.0825×10^{-11}.

[b]Uses only the available CC-CS rates; others set to zero.

[c]Uses CC-CS rates if available and generates the rest from the indicated extrapolation method.

List of Figures

FIG. 1. Difference between selected CS and IOS cross sections at 680 cm^{-1}.

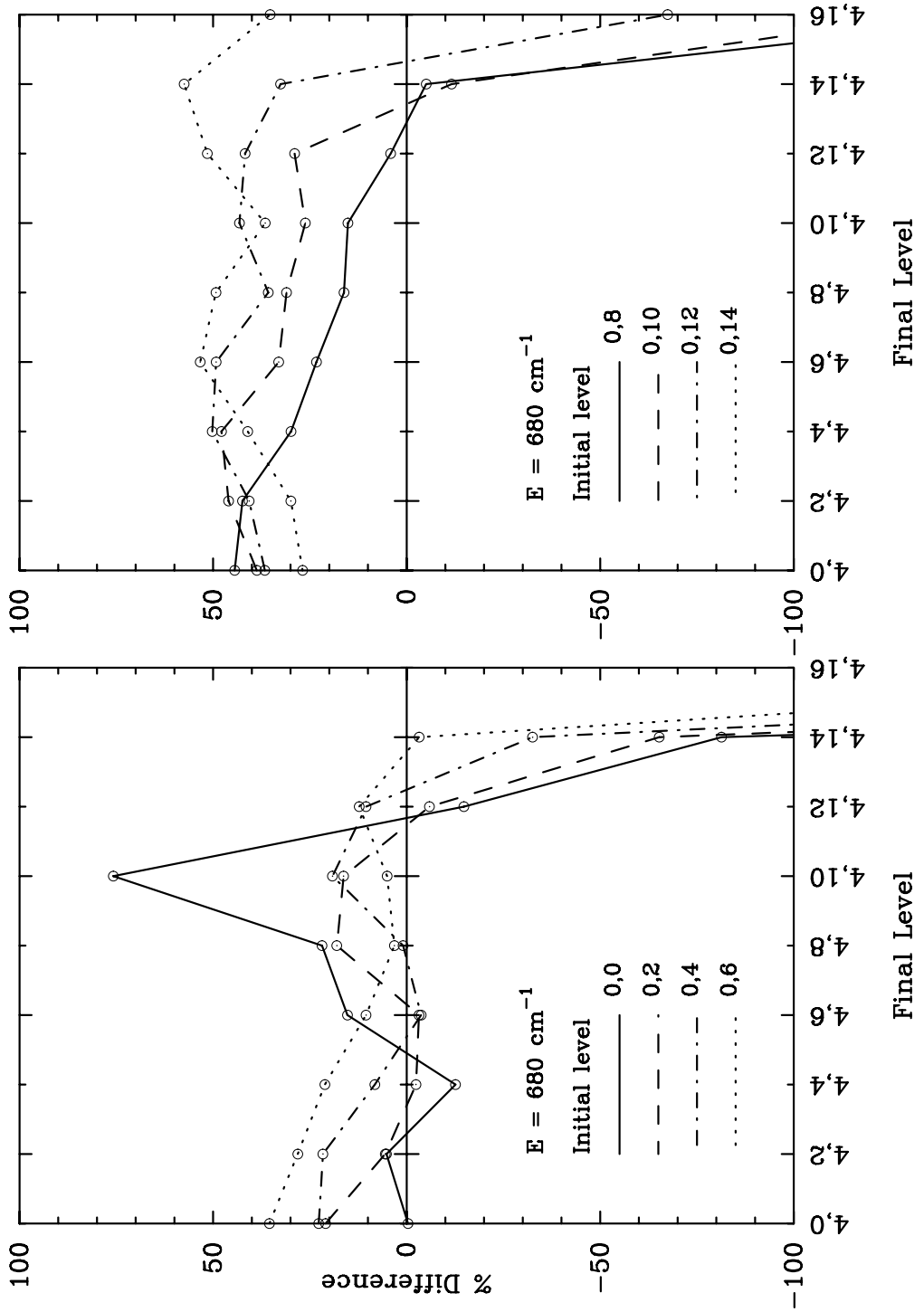

FIG. 2. Difference between σ^+ and σ^- calculated in the CC formulation at 219 cm^{-1}.

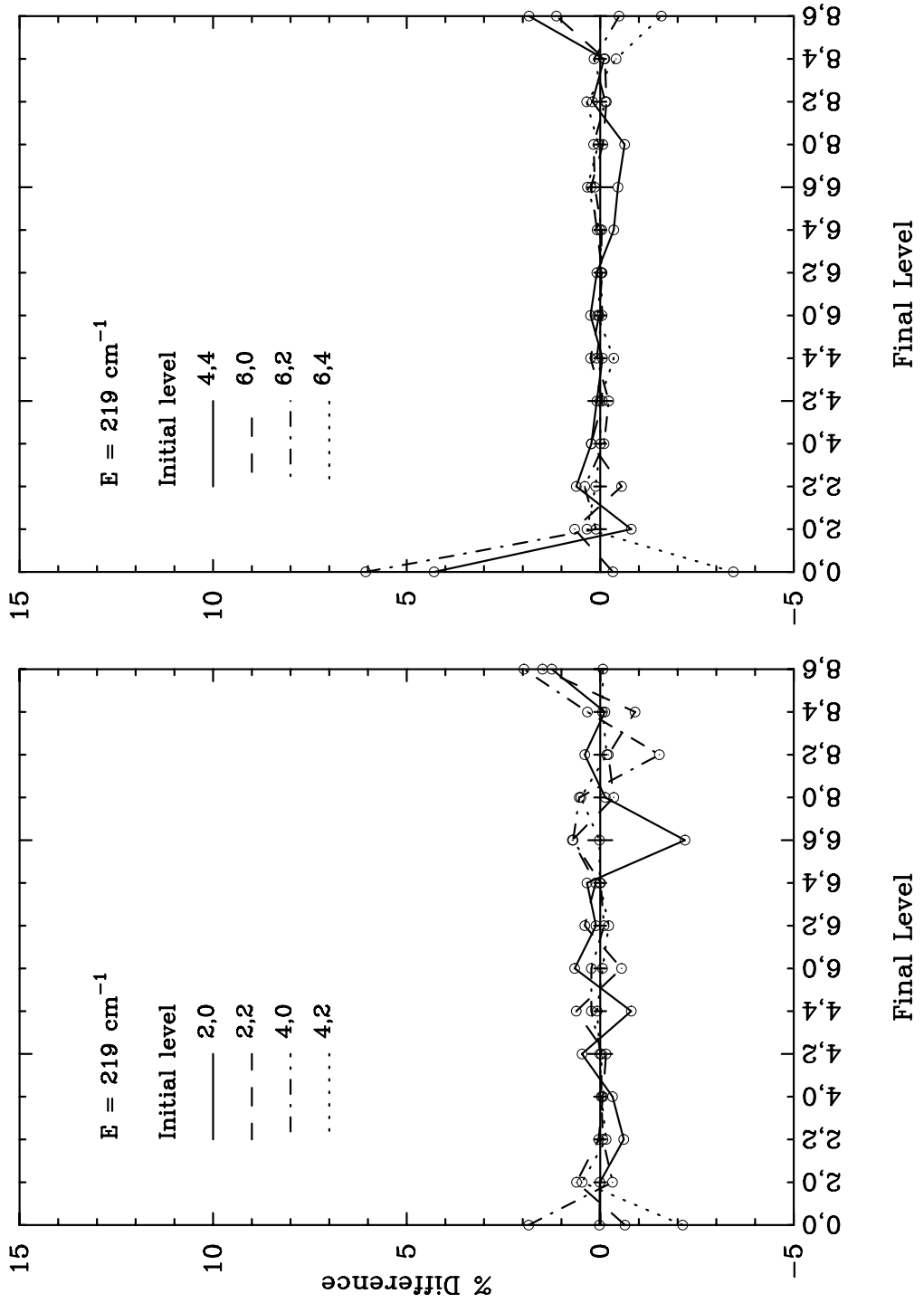

FIG. 3. Difference between the partial cross sections σ_J^+ and σ_J^- as a function of J for the (0,2) $\rightarrow$ (4,6) transition, calculated in the CC formulation at 219 $cm^{-1}$and in the CS approximation at 680 cm^{-1}.

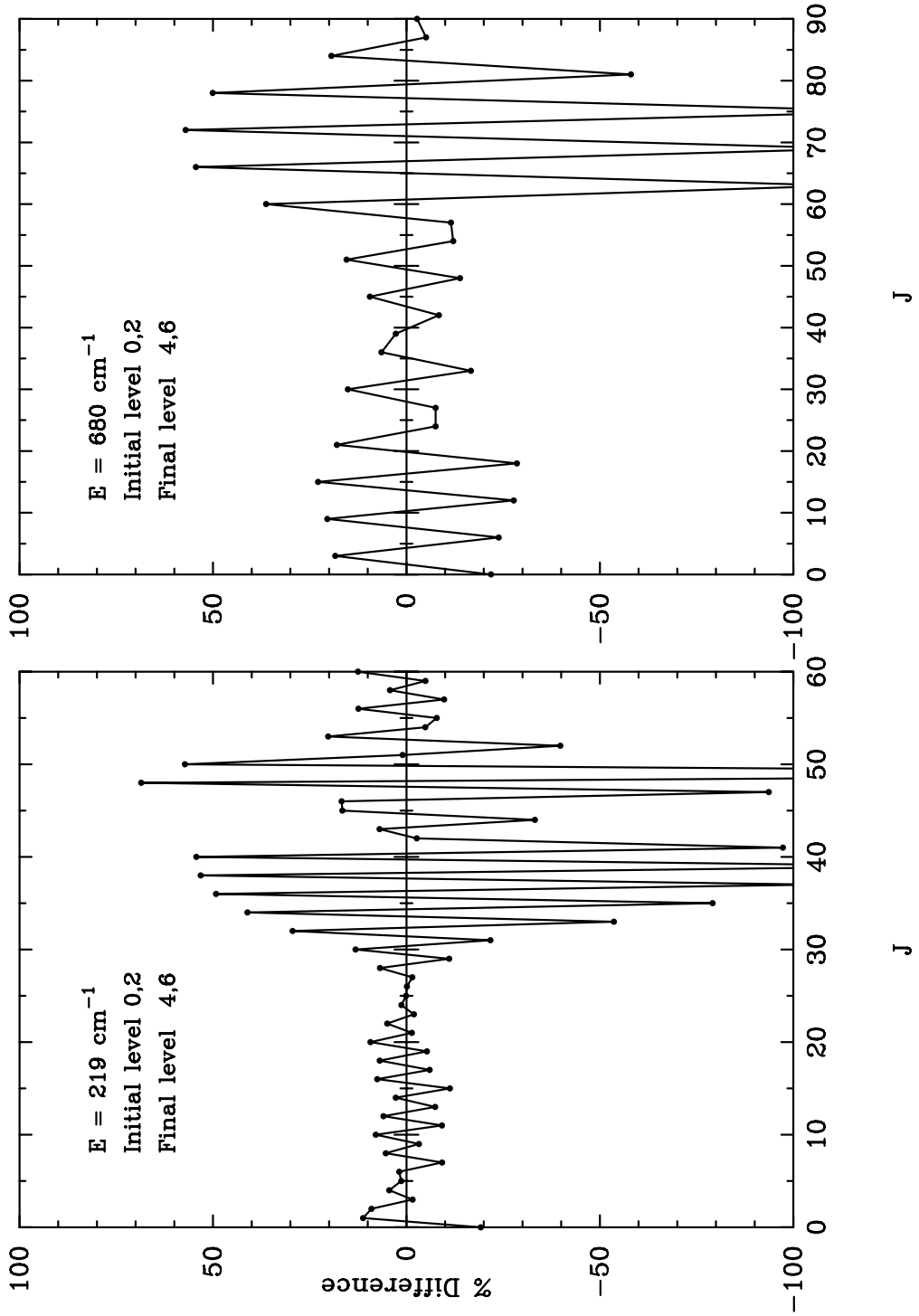

FIG. 4. Effective one-body rate constants for $j_i \rightarrow j_f$ from the coupled channel (CC-CS) calculations and from CC-CS augmented with extrapolations using the CSX and LSQ schemes are compared with the experimental data of Sitz and Farrow, Ref. [2].